

1 **Can the combining of wetlands with reservoir operation reduce the risk of future**  
2 **flood and droughts?**

3 Yanfeng Wu<sup>1</sup>, Jingxuan Sun<sup>1,2</sup>, Boting Hu<sup>1,2</sup>, Y. Jun Xu<sup>3</sup>, Alain N. Rousseau<sup>4</sup>, Guangxin Zhang<sup>1,\*</sup>

4 <sup>1</sup> Northeast Institute of Geography and Agroecology, Chinese Academy of Sciences, Changchun, Jilin  
5 130102, China

6 <sup>2</sup> University of Chinese Academy of Sciences, Beijing 100049, China

7 <sup>3</sup> School of Renewable Natural Resources, Louisiana State University Agricultural Center, 227 Highland  
8 Road, Baton Rouge, LA 70803, USA

9 <sup>4</sup> INRS-ETE / Institut National de la Recherche Scientifique - Eau Terre Environnement, 490 rue de la  
10 Couronne, G1K 9A9 Quebec City, Quebec, Canada

11 \* Correspondence: Professor Guangxin Zhang (zhgx@iga.ac.cn)

12  
13 **Abstract.** Wetlands and reservoirs are important water flow and storage regulators in a river basin;  
14 therefore, they can play a crucial role in mitigating flood and hydrological drought risks. Despite the  
15 advancement of river basin theory and modeling, our knowledge is still limited about the extent that  
16 these two regulators could have in performing such a role, especially under future climate extremes. To  
17 improve our understanding, we first coupled wetlands and reservoir operations into a semi-spatially  
18 explicit hydrological model and then applied it in a case study involving a large river basin in Northeast  
19 China. The projection of future floods and hydrological droughts was performed using the hydrological  
20 model during different periods (near-future: 2026-2050, mid-century: 2051-2075, and end-century:  
21 2076-2100) under five future climate change scenarios. We found that the risk of future floods and  
22 hydrological droughts can vary across different periods, in particular, will experience relatively large  
23 increases and slight decreases. This large river basin will experience longer duration, larger peak flows  
24 and volume, and enhanced flashiness flood events than the historical period. Simultaneously, the  
25 hydrological droughts will be much more frequent with longer duration and more serious deficit.  
26 Therefore, the risk of floods and droughts will overall increase further under future climate change even  
27 under the combined influence of reservoirs and wetlands. These findings highlight the hydrological

28 regulation function of wetlands and reservoirs and attest that the combining of wetlands with reservoir  
29 operation cannot fully eliminate the increasing future flood and drought risks. To improve a river basin's  
30 resilience to the risks of future climate change, we argue that implementation of wetland restoration and  
31 development of accurate forecasting systems for effective reservoir operation are of great importance.  
32 Furthermore, this study demonstrated a wetland-reservoir integrated modeling and assessment  
33 framework that is conducive to risk assessment of floods and hydrological droughts, which can be used  
34 for other river basins in the world.

35 **Keywords:** Climate change; Hydrologic projection; Floods and droughts; Wetland hydrological  
36 services; Reservoir operations; Model integration

37

## 38 **1. Introduction**

39 Floods and droughts have produced some of the most frequent and serious disasters in the world  
40 (Diffenbaugh et al., 2015; Hirabayashi et al., 2013; UNISDR, 2015). Globally, they account for 38% of  
41 the total number of natural disasters, 45% of the total casualties, more than 84% of the total number of  
42 people affected, and 30% of the total economic damage caused by all-natural disasters (Güneralp et al.,  
43 2015) in the past. As climate change has been accelerating the hydrological cycle, causing more frequent  
44 and stronger weather extremes, more floods and droughts have been projected to increase at both global  
45 (Chiang et al., 2021; Jongman, 2018) and regional scales (Hallegatte et al., 2013; Wang et al., 2021).  
46 Concurrently, the disaster-related loss of ecosystems (e.g., wetlands, forest, and grassland) and their  
47 services can mitigate the flood and drought risks to a great extent (Gulbin et al., 2019; Walz et al., 2021).  
48 Given this, grey infrastructure such as dams, dikes, and reservoirs, which have often been used to  
49 attenuate flood and drought hazards because of their rapid and visible effects, can play an important role  
50 in ensuring the water security of a river basin (Alves et al., 2019; Casal-Campos et al., 2015). However,  
51 relying solely on grey infrastructure to attenuate floods and droughts has some inadequacies, such as  
52 large investments to build and maintain in addition to adverse effects on downstream ecosystems (Maes  
53 et al., 2015; Schneider et al., 2017). In this context, Nature-based solutions (NBS) for hydro-

54 meteorological hazards mitigation are becoming increasingly popular (Kumar et al., 2021), because  
55 NBS can effectively reduce or even offset the hydrological processes driving floods and droughts (Nika  
56 et al., 2020), while making least disturbance to the environment as well as delivering co-benefits which  
57 grey infrastructure cannot provide (Anderson and Renaud, 2021; Nelson et al., 2020). Therefore, it is  
58 urgent to integrate NBS into the current water management practices to increase basin resilience to  
59 hydrological extremes under climate change.

60 Wetlands have the potential to be used as a NBS for improving water storage and hence the resilience  
61 of a river basin to hydrological extremes along with grey infrastructures (Thorslund et al., 2017). This  
62 is because, similar to man-made dams and reservoirs, wetlands can attenuate flow and alter basin  
63 hydrological processes (Lee et al., 2018), such as floods (Wu et al., 2020a) and baseflows (Evenson et  
64 al., 2015; Wu et al., 2020b). However, unlike man-made grey infrastructures, wetlands are integral in  
65 landscapes and they are connected laterally and vertically with the surrounding terrestrial and aquatic  
66 environments through the hydrological cycling of water and waterborne substances (Åhlén et al., 2020),  
67 making their water storage and cycling fundamental to estimate a watershed's water balance (Golden et  
68 al., 2021; Shook et al., 2021). To understand how and to what extent wetlands can mitigate hydrological  
69 processes, two approaches are commonly used: (i) description of individual wetland services at the field  
70 scale (e.g., Park et al., 2014) or wetlandscape scale (e.g., Åhlén et al., 2022); (ii) assessment of wetland  
71 hydrological services at the regional/watershed scale (Fossey et al., 2016; Wu et al., 2020a, 2020b).  
72 However, the former approach can only be achieved with field observation with instruments and is  
73 mainly used to provide key parameters of wetland processes for model calibration (Fossey and Rousseau,  
74 2016). Recently, several wetland modules have been development and coupled to hydrological (e.g.,  
75 Soil and Water Assessment Model, HYDROTEL model) to quantify hydrological function of wetlands,  
76 particularly the mitigation services on floods and droughts (Evenson et al., 2018; Evenson et al., 2016;  
77 Fossey et al., 2015; Zeng et al., 2020). These wetland hydrological models not only consider the general  
78 water budget of a river basin but also consider the perennial and intermittent hydrological interactions  
79 between wetlands-to-wetlands and wetlands-to- surrounding landscapes. It is of both scientific and  
80 practical interest to project wetland capability in mitigating floods and droughts in response to a

81 changing climate.

82 Reservoirs redistribute large amounts of surface water, thus altering natural hydrological processes,  
83 such as flow range, flood and drought patterns, and basin water balances (Boulangue et al., 2021; Chen  
84 et al., 2021; Manfreda et al., 2021; Zhao et al., 2016). So far, throughout the world, there are 57, 985  
85 reservoirs registered by the International Commission on Large Dams and their total volume has been  
86 reached 14, 602 km<sup>3</sup> (Eriyagama et al., 2020). Such numerous reservoirs and their large storage capacity  
87 should not be neglected in water hazard assessment and hydrological projection because of their  
88 significant modification on flood and drought patterns (Boulangue et al., 2021; Brunner et al., 2021). For  
89 that reason, scholars called for the need to integrate reservoirs in model-based impact analysis of flood  
90 exposure under climate change (Dang et al., 2020a; Yassin et al., 2019). Therefore, there is a growing  
91 need in incorporating reservoir operations into basin hydrologic simulations and predictions.

92 Despite the well-established knowledge of flow regulation and water storage functions that wetlands  
93 and reservoirs can provide in a river basin, most modeling assessments on floods and droughts at the  
94 basin scale do not take the two components into account, or give little emphasis on the combined benefits  
95 of them (Brunner et al., 2021; Golden et al., 2021). Nor are the hydrological processes associated with  
96 these features implicitly included in the calibration of hydrologic models. Recent studies have suggested  
97 that disregarding of the wetlands or reservoir operation would add significant error and larger  
98 uncertainties to simulate hydrologic processes (Brunner et al., 2021; Ward et al., 2020). Because  
99 wetlands are often abundant across many landscapes, which make their water storage and cycling  
100 fundamental to estimate a watershed's water balance (Rains et al., 2016; Lee et al., 2018). Therefore,  
101 missing this component of water balances could potentially lead to disproportionately large model errors  
102 (Rajib et al., 2020). Consequently, integrating the wetlands (Fossey et al., 2015; Golden et al., 2021;  
103 Rajib et al., 2020) or reservoir operation (Dang et al., 2020; Yassin et al., 2019; Zhao et al., 2016) alone  
104 into watershed-scale hydrologic models may largely minimize uncertainties and improve model  
105 performance. Furthermore, on a global scale, most river basins have wetlands and their river flow has  
106 or will experience reservoir regulation (Muller, 2019; Schneider et al., 2017), which elicits thought-  
107 provoking concerns: What will be the changes of future floods and droughts under the combined

108 influence of wetlands and reservoirs? Such concern is important because the omission of wetlands and  
109 reservoirs can cause the policy-making process to be imprecise at best and ineffective at worst. However,  
110 a reservoir operation and wetland services, integrated basin-scale model rarely exist in the literature.  
111 Furthermore, although few studies (e.g., Rajib et al. (2020; Chen et al., 2021; Wu et al., 2021) provide  
112 insights into modeling and understanding the flow regulation functions provided by wetlands and  
113 reservoirs, however, is it still unclear whether the combining of wetlands with reservoir operation can  
114 largely reduce the risk of future floods and droughts.

115 Considering the above-introduced scientific challenges and management deficiencies, we first  
116 developed a framework of hydrological modeling coupled with wetland modules and reservoir operation  
117 scenarios. We then applied it to a large river basin with abundant wetlands and a large reservoir, the  
118 Nenjiang River Basin in northeast China, to address a central question: Can the combining of wetlands  
119 with reservoir operation largely reduce the risk of future flood and droughts? The Nejinang River Basin  
120 was selected as a case study here because it has abundant wetlands and a large reservoir, and has  
121 undergone intensive anthropogenic activities in the past half century, particularly in the increasing  
122 agricultural water consumption and conversion of wetlands to agricultural and other land uses. Our  
123 framework and results are expected to bring new insights into future floods and droughts and provide a  
124 basis for decision-making to curb the growing impacts of unprecedented and future hydrological  
125 extreme conditions.

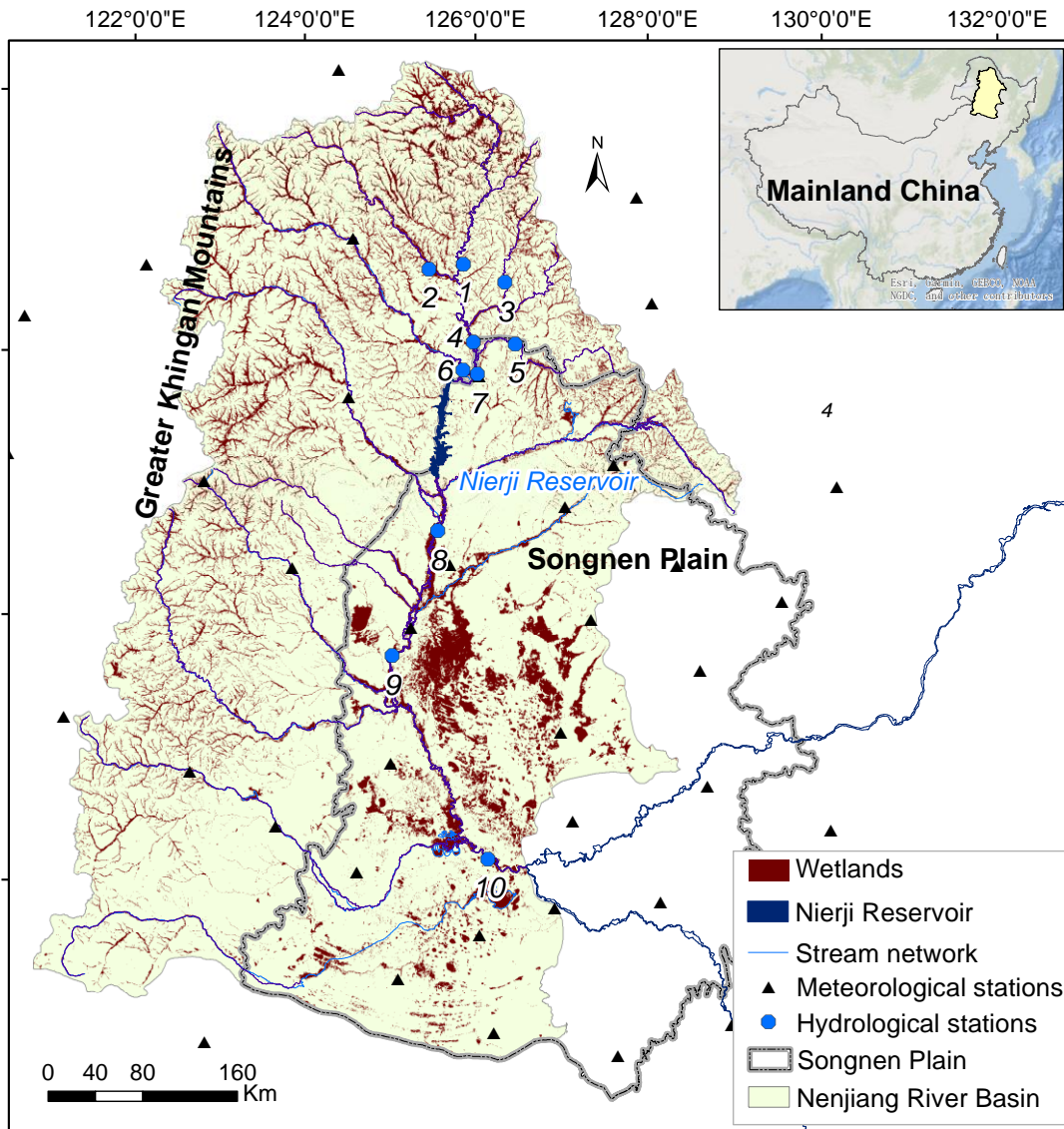
## 126 **2. Methodology**

### 127 2.1 Study area and datasets

128 We conducted this analysis in the Nenjiang River Basin (NRB), a large river basin (291,700 km<sup>2</sup>)  
129 located in the Northeast China (Fig. 1). Long-term annual average runoff depth and volume from the  
130 NRB are 97.4 mm and 22.7 billion m<sup>3</sup>. The river basin is located in the middle-high latitudes and can  
131 be characterized by a temperate semi-humid continental monsoon climate. Inter-annual differences in  
132 temperature and precipitation are large, i.e., disparate hot and cold periods, and uneven dry and wet  
133 conditions (Meng et al., 2019). The average annual temperature across the basin ranges between 2.1-

134 4.5°C. The annual total precipitation within the basin fluctuates from 323.1 to 537.6 mm. Precipitation  
135 is mainly concentrated during June-September, which accounts for about 85% of the annual  
136 precipitation (Li et al., 2014).

137 The NRB is one of the pivotal wetland areas in China. The basin contains several important wetland  
138 conservation areas, among which Zhalong and Nanweng River Wetlands have been designated as a  
139 Ramsar Site of International Importance. The wetlands and their contributing drainage areas (see  
140 Section 2.2.1 for specific definition) within the subbasins monitored by the ten hydrological stations  
141 range from 14 to 23% and from 39 to 56% respectively, demonstrating the large wetland coverage of  
142 the NRB and its sub-basins (Table 1). The lower NRB is an important agricultural area of the Songnen  
143 Plain, which is one of the three major plains (including the Sanjiang, Songnen and Liaohe Plains) in  
144 northeast China. Therefore, understanding potential floods and hydrological droughts under future  
145 climate change is crucial for ensuring regional food security and wetland ecological integrity. During  
146 the past 60 years, land use and land cover types have drastically changed owing to large-scale  
147 development of intensive agriculture and water resources management (Meng et al., 2019). The area of  
148 wetlands in the NRB decreased by nearly 23% from 1978 to 2000 (Chen et al., 2021), with only 16.34%  
149 remaining today (Table 1), which largely degraded their services (Wu et al., 2021). Along with the  
150 reduction in wetland area, the hydrological functions of wetlands in the NRB, such as water storage,  
151 flood mitigation and baseflow support, have been considerably reduced (Wu et al., 2021). These wetland  
152 services are closely related to flood and drought risks, such as the 1998 mega-flood. In order to  
153 effectively deal with the risk of floods and droughts, the Nierji Reservoir was constructed along the  
154 mainstream NRB (Fig. 1); it started normal operation in 2006. The drainage area of the reservoir  
155 accounts for 22.8% of the NRB. The Nierji Reservoir, located in the upper Nenjiang River (Fig. 1), has  
156 flood control and water supply as the primary purposes and hydropower generation and navigation as  
157 secondary purposes, thus playing an important role in the distribution of water resources for the lower  
158 NRB.



159  
 160 Figure 1. Location of the Nenjiang River Basin and the distribution of wetlands, river networks, Nierji  
 161 Reservoir, and hydrological and meteorological stations within the basin.

162  
 163 Table 1. The drainage area of the ten hydrological stations used in this study, area ratios of wetlands  
 164 and their contributing areas to the drainage area of the Nenjiang River Basin, northeast China.

ID	River	Hydrological stations	Drainage area (km <sup>2</sup> )	Wetland area ratio (%)	Wetland contribution area ratio (%)
1	Mainstream	Shihuiyao	17205	22.2	54.7

2	Duobukuli River	Guli	5490	16.3	57.1
3	Menlu River	Huolongmen	2151	20.8	50.7
4	Mainstream	Kumotun	32229	20.4	54.3
5	Keluo River	Kehou	7310	23.4	56.2
6	Gan River	Liujiatun	19665	13.2	49.9
7	Mainstream	Nenjiang	61249	18.3	54.1
8	Mainstream	Tongmeng	108029	13.1	47.5
9	Mainstream	Fulaerji	123911	13.7	39.0
10	Mainstream	Dalai	221715	16.3	42.4

165

166 The driving datasets used in this study include meteorological data, land-use/land-cover types, soil  
167 texture, digital elevation models, drainage network, and observed discharge data. The land-use/land-  
168 cover types for 2015 (including wetland types), digital elevation models and digital elevation models  
169 with 1 km resolution were obtained from Resource and Environment Science and Data Center  
170 (<https://www.resdc.cn/>). The river network was collected from the Geographical Information  
171 Monitoring Cloud Platform (<https://www.dsac.cn/DataProduct/Index/30>). Historical daily  
172 meteorological datasets including precipitation and air temperature for the period 1963-2020 were  
173 obtained from 39 weather stations administered by the National Meteorological Information Centre of  
174 China (<http://data.cma.cn>) and 49 weather stations in the upper NRB (Fig. 1) administered by the  
175 Nenjiang Nierji Hydraulic and Hydropower Ltd. Company (<http://www.cnnej.cn>). The hydrological  
176 data from ten hydrological stations (see Fig.1 and Table 1) were obtained from the Songliao Water  
177 Resources Commission, Ministry of Water Resources (<http://www.slwr.gov.cn/>), with the time series  
178 extending from 1963 to 2020.

179 In this study, we drove hydrological model using five GCM projections (GFDL-ESM4, IPSL-CM6A-  
180 LR, MPI-ESM1-2-HR, MRI-ESM2-0, UKESM1-0-LL) under three Socioeconomic Pathways (SSPs)  
181 from the latest CMIP6 (O'Neill et al., 2016). Each of these specific SSPs represents a development  
182 model that includes a corresponding combination of development characteristics and influences. The



183 three SSPs that were used herein include SSP126, SSP370 and SSP585, which represent potential  
184 futures characterized by green-fueled growth (van Vuuren et al., 2017), high inequality between the  
185 countries (O'Neill et al., 2016) and fossil-fueled growth (Kriegler et al., 2017), respectively. We chose  
186 the five GCM projections because their high resolution (0.25°) and wide application in previous studies.  
187 Given the data requirements of the hydrological model, we downloaded the SSP outputs including daily  
188 precipitation, maximum and minimum temperature. We then performed bias correction and spatial  
189 downscaling of the SSP outputs. The bias correction of SSP outputs was carried out using the CMhyd  
190 software (<https://swat.tamu.edu/software/cmhyd>), in which the widely used Delta Change method in the  
191 CMhyd software was adopted. Delta Change bias-corrects the projected SSP outputs based on the  
192 historical statistics and thus conserves the linear spatial-, temporal-, and multi-variable dependence  
193 structure in the future climate (Bosshard et al., 2011; Maraun, 2016; Moore et al., 2008; Shafeeque and  
194 Luo, 2021). The ANUSPLIN package developed by (Hutchinson and Xu, 2004) was then used to  
195 uniformly downscale the output from five bias-corrected GCMs to a resolution of 1-km based on the  
196 DEM. Following previous studies (Hagemann and Jacob, 2007; Zhao et al., 2021), the multi-model  
197 ensemble means ( $M_{GCM}$ ) of the daily precipitation, and the maximum and minimum temperature under  
198 the SSPs scenarios were then obtained to diminish the uncertainties inherited in a single GCM. MEM  
199 was calculated using an equally-weighted average:

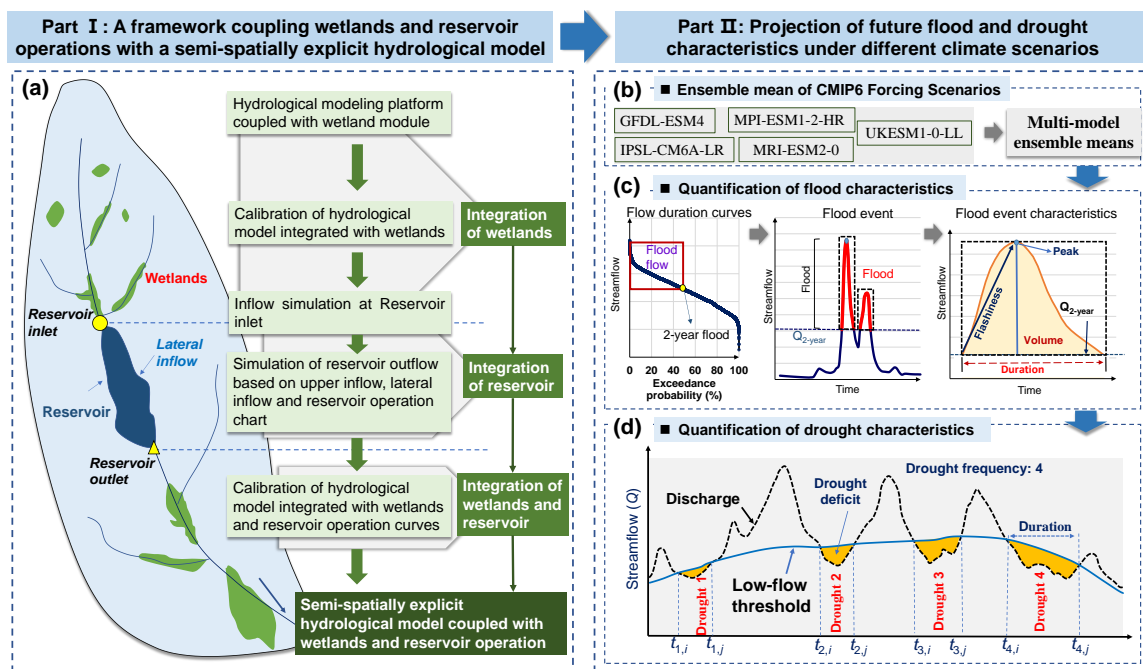
$$200 \quad M_{GCM} = \frac{1}{N} \sum_{i=1}^N P_i \quad (1)$$

201 where  $M_{GCM}$  is the multi-model ensemble means,  $N$  is the number of ensemble members (5 in this study);  
202 and  $P_i$  is the projected climate data of an ensemble member. In this study, the  $M_{GCM}$  of five GCMs were  
203 used to drive hydrological modeling.

## 204 2.2. Framework of hydrological modeling coupled with wetland modules and reservoir operation 205 scenarios

206 We developed a spatially-explicit hydrological modeling framework that considers wetland  
207 hydrological processes and reservoir operations based on HYDROTEL model and reservoir simulation  
208 algorithms (Fig.2). Such a modeling framework was based on a distributed coupling implementation at

209 watershed scale from upstream to downstream. Observed streamflow from seven hydrological stations  
 210 (see hydrological stations 1-7 in Fig.1) located upstream of the Nierji Reservoir and three hydrological  
 211 stations (see hydrological stations 8-10 in Fig.1) installed at downstream of the reservoir, respectively,  
 212 were used to calibrate the HYDROTEL model. For the upstream Nierji Reservoir, we calibrated the  
 213 HYDROTEL model against observed streamflow of seven hydrological stations with consideration of  
 214 wetlands (i.e., hydrologic-wetlands model). Among the seven hydrological stations, the Nenjiang  
 215 Station is located at the end of the upstream, where the simulated streamflow was taken as the inflow of  
 216 the reservoir. We then computed the reservoir outflow using the simulated inflow, estimated lateral  
 217 inflow and reservoir simulation algorithms (see Section 2.2.2), thereby integrating reservoir operation  
 218 into the hydrologic-wetlands model to build a hydrologic-wetlands-reservoir model. Based on the  
 219 calibrated hydrologic-wetlands-reservoir model, we simulated the outflow of the reservoir (Sect. 2.2.2),  
 220 which was used as the input streamflow for downstream model calibration. For the downstream reservoir,  
 221 we calibrated the hydrologic-wetlands-reservoir model against observed streamflow of Tongmeng,  
 222 Fulaerji and Dalai Stations. Based on this framework, the simulation of basin hydrological processes  
 223 coupled with basin scale wetlands and reservoir operations were realized.



224  
 225 Figure 2. Framework for projecting future flood and hydrological droughts based on a semi-spatially

226 integrating wetlands and reservoir operation into a basin hydrological model: (a) a framework coupling  
227 wetlands and reservoir operations with a semi-spatially explicit hydrological model; (b) multi-model  
228 ensemble means from five GCM projections used for driving modeling framework; (c) methodology  
229 for determining a flood threshold, defining flood events, and extracting flood characteristics, and (d) a  
230 sequence of runs with examples of drought deficit, duration, and frequency.

#### 231 2.2.1. A semi-distributed hydrological model platform coupled with wetland modules

232 The PHYSITEL/HYDROTEL modeling platform coupled with two wetland modules (isolated and  
233 riparian wetlands) (Fossey et al., 2015), has been used to quantify hydrological function of wetlands  
234 (e.g., Fossey and Rousseau, 2016; Blanchette et al., 2019; Wu et al., 2023). PHYSITEL is a Geographic  
235 Information System based pre-processing platform for managing hydrological modeling data (Noël et  
236 al., 2014; Rousseau et al., 2011). Using general basin data (a digital elevation model, vectorized river  
237 network and lacustrine water bodies, and raster-based land use and soil matrix distribution maps),  
238 PHYSITEL divides the basin into more detailed hydrological response units, i.e., relatively  
239 homogeneous hydrological units (RHHUs) (Fortin et al., 2001). The RHHUs were defined using the  
240 algorithm for delineating and extracting hillslopes proposed by (Noël et al., 2014). The hillslopes with  
241 same characteristics (e.g., physical geography and hydrological response) were then aggregated within  
242 each RHHUs. In addition, the PHYSITEL platform distinguishes wetlands from other land-use types,  
243 and then classifies both isolated and riparian wetlands based on an adjacency threshold (i.e., percentage  
244 of pixels in contact) between the wetlands and the river network (Fossey et al., 2015). Specifically, if  
245 more than adjacency threshold (e.g., 1%) of wetland pixels are connected to the river network, they are  
246 considered as pixels of a riparian wetlands; otherwise, they are referred to as isolated wetlands. It  
247 subsequently generates data pertaining to isolated and riparian wetlands and their contributing areas.  
248 The contributing area of wetlands is defined as the sum of the area of all wetland RHHUs and upland  
249 RHHUs within their immediate catchment areas situated along active fill-spill pathways to the stream  
250 network (Evenson et al., 2016). The PHYSITEL platform uses the concept of a hydrologically  
251 equivalent wetland (HEW) proposed by (Wang et al., 2008) to integrate isolated and riparian wetlands  
252 at the RHHU scale. These typically large RHHUs contain large wetland complexes consisting of various

253 wetland categories such as bogs, fens, marshes, and forested peatlands. After defining the hydrological  
254 and wetland parameters, PHYSITEL can directly export the database as part of the input data to  
255 HYDROTEL; these data can also be used for other watershed hydrological models.

256 HYDROTEL is a physically-based and semi-distributed hydrological model (Bouda et al., 2014;  
257 Bouda et al., 2012; Turcotte et al., 2007) that requires wetland parameter data, land-use type maps, soil  
258 texture maps, meteorological data (e.g., daily temperature and precipitation) and daily flows as input.  
259 The HYDROTEL model couples the hydrological processes associated with both isolated and riparian  
260 wetlands (i.e., the isolated and riparian wetlands modules) at the RHHU scale and calculates the wetland  
261 water balance with respect to the surface area of the HEW, contribution area and RHHU. Specifically,  
262 for isolated wetlands, the hydrogeological processes are integrated in the vertical water budget (Fortin  
263 et al., 2001) at the RHHU scale. For riparian wetlands, the water balance is partially integrated in the  
264 vertical water budget of an RHHU and directly connected to the associated river segment via the  
265 kinematic wave equation (Beven, 1981). Based on this, the isolated wetlands modules can realize the  
266 vertical water balance processes of hillslope wetlands with land surface runoff processes, while the  
267 riparian wetlands modules can realize the interaction of hydrological processes between riparian  
268 wetlands and river channels. It should be mentioned that the HEW concept developed by Wang et al  
269 (2008) served as the foundation for the integration of riparian wetlands and isolated wetlands into the  
270 modeling framework. This concept contends that the features of one HEW (also known as an isolated  
271 wetland or riparian wetland) are equivalent to the sum of the characteristics of each wetland inside a  
272 RHHU (which could either be hill slopes or elementary sub-watersheds related to one river segment).  
273 The following premises apply to this concept: (i) only one isolated and/or riparian HEW per RHHU; (ii)  
274 one HEW can be fully integrated within a RHHU; (iii) isolated HEW parameters must be numerically  
275 integrated; and (iv) riparian HEW parameters must be numerically integrated and spatially integrated  
276 (i.e., located in a specific location on the river segment). Therefore, isolated wetlands and riparian  
277 wetlands do not appear to have direct hydrological connection within a RHHU. However, isolated  
278 wetlands also have hydrological interactions with riparian wetlands through vertical water balance  
279 processes and fill-spill processes (Fossey et al., 2015). Nevertheless, such representations provide a

280 modelling approach that can simulate water balances at the wetland scale while considering their  
281 interactions with the surrounding environment (contributing drainage area and hydrological  
282 connectivity) (Fossey et al., 2015). But the hydrological interactions between riparian wetlands and  
283 isolated wetlands are not considerate in this study.

#### 284 2.2.2. Simulation of Nierji reservoir operations

285 Based on the simulated runoff at the inlet (the Nenjiang Station), lateral inflow, and the schemes of  
286 reservoir operation, we estimated the reservoir outflow using the ResSimOpt-Matlab software package  
287 developed by Dobson et al., 2019. ResSimOpt-Matlab contains three algorithms for reservoir simulation.  
288 The first algorithm considers a case when we want to always release a constant amount over the  
289 simulation period. This constant amount is the target release that would cover all downstream demand  
290 for water, for instance for domestic use and/or irrigation. The second consider a case when we still want  
291 to release the target demand but we would also like to (1) apply some hedging (that is, an intentional  
292 reduction of the release - even if it would still be feasible to release the target demand - aimed at saving  
293 more water and thus facing smaller deficits at later time); and (2) attenuate downstream peak flows for  
294 flood control purpose. The third algorithm, which was used in this study, dynamizes the operation rules.  
295 A dynamic operation schemes was used in this study to achieve the simulation. Specifically, following  
296 (Dobson et al., 2019) and according to actual hydrological conditions, we defined two seasons: the wet  
297 season (from June to September) when the risk of flooding is higher and we wanted to release the target  
298 demand and provide some storage space for flood control, and the dry season when the risk of flooding  
299 is low and the main objective is to sustain ecological baseflows. The required input data to the algorithm  
300 includes reservoir inflow ( $Q_{in}$ ) ( $m^3/s$ ), the minimum environmental flow ( $E_{env}$ ), ( $m^3/s$ ) initial storage ( $S_o$ )  
301 ( $m^3$ ), minimum ( $S_{min}$ ) and maximum ( $S_{max}$ ) storage ( $m^3$ ), estimated evaporative losses ( $E_{vap}$ ) (mm),  
302 released discharge ( $Q_{out}$ ) ( $m^3/s$ ) and the simulation time-step length (day). Based on the required data,  
303 we performed reservoir simulation by implementing the mass balance equation at each simulation time  
304 step  $t$ :

$$\begin{cases}
S_{(t+1)} = S_{(t)} + Q_{in(t)} - E_{vap(t)} - Q_{out(t)} & \text{or} & S_{(t)} + Q_{in(t)} - E_{min(t)} - E_{vap(t)} \\
0 \leq S_{(t)} \leq S_{max} \\
0 \leq R_{(t)} \leq \min(S_{(t)} + Q_{in(t)} - E_{min(t)} - E_{vap(t)}, Q_{max})
\end{cases} \quad (2)$$

306 where  $S_t$  is the reservoir storage at time  $t$ .  $S_t$  and  $Q_{out}$  are constrained by the design specifications  
307 and operation rules of a reservoir. Specifically,  $S_t$  cannot exceed the reservoir capacity  $S_{max}$ , while  
308  $Q_{out}$  ( $m^3/s$ ) is constrained by the operation schemes and capacity of the turbines  $Q_{max}$  ( $m^3/s$ ). The  
309 excess water, if any, is spilled:

$$Q_{spill(t)} = \max(S_{(t)} + Q_{in(t)} - E_{vap(t)} - Q_{out(t)}) \quad (3)$$

311 Based on this, the dynamic  $Q_{out}$  can be represented using the equation (1) and (2).

312 We collected information on the reservoir operation including reservoir capacity, control water levels,  
313 outflow, the storage-area-water level relationship, the tailwater level-discharge relationship, and the  
314 maximum release, along with other data necessary to estimate the outflow. The reservoir inflow is the  
315 simulated streamflow at the Nengjiang Hydrological Station, which is at the inlet of the Nierji Reservoir.  
316 The minimum storage and maximum storage are 4.9 billion  $m^3$  and 86.1 billion  $m^3$ , respectively. Based  
317 on the available data for the study area, the Karrufa method (Kharrufa, 1985) was used to estimate daily  
318 evaporative losses from the reservoir. We convert days to seconds so that it would correspond to the  
319 flow data. During the wet season, the actual operation schemes for the Nierji Reservoir are as follows:  
320 The pre- and post-flood periods are June 1-20 and September 6-30, respectively, with a flood limited  
321 water level of 216.0 m; The main flood period is from June 21 to August 25, and the reasonable flood  
322 limited water level ranges from 213.4 m to 216.0 m and can be gradually increased. During the dry  
323 season, the environmental flow was defined as 25.3% of the daily streamflow during the dry season  
324 over the years based on the designed operating curves of the reservoir operation chart.

### 325 2.2.3. Model calibration, validation and performance assessment

326 For all above scenarios, we calibrated the HYDROTEL model against observed streamflow at a daily  
327 time step over 8 years, including a 1-year warm-up (2010.10.01-2011.09.30) and a 7-year calibration  
328 (2011.10.01-2018.09.30) periods. The same model settings (i.e., key parameters, simulation periods,

329 fitting algorithm, and objective function, etc.) were used for the calibration processes under the both  
330 presence and absence scenarios. Following (Arsenault et al., 2018), the model was calibrated using full-  
331 time observations without additional validation, as the former allows for more reliable parameters and  
332 maximizes the accuracy of the model. The dynamically dimensioned search algorithm (DDS) developed  
333 by (Tolson and Shoemaker, 2007) was used to calibrate the 13 most sensitive parameters of the model  
334 as proposed by (Foulon et al., 2018). Based on the maximizing of Kling-Gupta efficiency (KGE) (Gupta  
335 et al., 2009), automatic calibrations using DDS were carried out utilizing 10 optimization trials (250 sets  
336 of parameters per trial). Then, the best set of parameter values out the 10 trials were selected following  
337 (Foulon et al., 2018). The KGE was chosen as the objective function because previous research has  
338 shown that it can improve flow variability estimates when compared to the Nash-Sutcliffe efficiency  
339 (NSE) (Fowler et al., 2018; Garcia et al., 2017).

340 It should be noted that we calibrated the HYDROTEL model against observed streamflow under with  
341 and without wetland scenarios. For the without wetland scenarios are defined as follows: When the  
342 wetland modules are turned off in HYDROTEL, wetland areas are not removed, but they are treated as  
343 the land cover of saturated soils. Such a saturated soil is fixed and does not participate in hydrological  
344 processes such as water yielding and runoff routing, and thus their explicit storage properties are not  
345 accounted for in the modeling. This is a basic assumption that has been used in several studies using  
346 models such as SWAT (Liu et al., 2008; Wang et al., 2008; Evenson et al., 2015), Mike 11 (Ahmed,  
347 2014) and HYDROTEL (Fossey et al., 2016; Fossey and Rousseau, 2016a, b; Wu et al., 2019, 2020a,  
348 2021), to quantify the hydrologic services provided by wetlands (flood mitigation, flow regulation and  
349 baseflow support etc.).

350 To determine whether coupling the wetland module and the reservoir can improve the model  
351 performance, we compared (1) the efficiency of the model in simulating daily flow processes; and (2)  
352 the capability of the model to simulate floods and hydrological droughts in the presence or absence of  
353 the wetlands and the combination of wetlands and reservoir. Following the recommendations of (N.  
354 Moriasi et al., 2007) and (Moriasi et al., 2015), four performance criteria were selected to assess model  
355 performance with regards to simulated daily flows with and without the presence of the wetland modules

356 and reservoir operation, namely the NSE (Nash and Sutcliffe, 1970), Correlation Coefficient (CC), the  
357 root-mean square error (RMSE) and the percent bias (Pbias). We used multiple performance criteria  
358 because it may be unreliable to rely on a single objective function to determine whether the model  
359 performs well (Fowler et al., 2018; Pool et al., 2018; Seibert et al., 2018). It should be noted that although  
360 NSE as an objective function has shortcomings in model calibration, it can still provide an important  
361 reference for the evaluation of simulation results as a performance criterion as suggested by Moriasi et  
362 al. (2007, 2015). In addition, we compared model performance considering daily hydrograph changes.  
363 Furthermore, flood and drought features were extracted (see Sect. 2.4.2 and 2.4.3) and used to discern  
364 whether, and to what extent, the coupled wetland modules and reservoir simulations could improve the  
365 model's ability to simulate droughts and floods.

366

### 367 2.3. Projection of future flood and drought characteristics under different climate scenarios

368 The calibrated hydrologic-wetland-reservoir model was used to simulate streamflow driven by multi-  
369 model ensemble means from the latest CMIP6 and to derive drought and flood characteristics. The flood  
370 and drought characteristics were then compared against historical periods (1971-2020) to discern how  
371 future hydrological extremes will be changed under the influence of wetlands and reservoirs (see Part  
372 II in Fig.2).

373 The future simulated streamflow at the Nenjiang and Dalai hydrological stations driven by the  
374 ensemble mean of bias-corrected CMIP6 Forcing Scenarios (see Section 2.1) were selected to derive  
375 drought and flood characteristics. The Nenjiang Station was chosen because it is located at the outlet to  
376 (mouth of) the upper NRB and the inlet to the Nierji Reservoir, whose flood and drought patterns are  
377 mainly driven by wetlands and climate change. Moreover, changes in drought and flood characteristics  
378 of the Nenjiang Station are critical to the operation of the reservoir immediately lower reach. The Dalai  
379 Station, located at the outlet of the entire NRB, was used as a proxy to characterize future flood and  
380 drought evolution for the whole basin under the combined influence of the wetlands and reservoir. Using  
381 the calibrated hydrologic-wetland-reservoir model, we carried out the simulation of hydrological  
382 processes for the historical period and under the constraints of the SSP126, SSP370 and SSP585



383 scenarios. We then extracted flood and hydrological drought characteristic indices from the simulations  
384 to conduct a comparative analysis of their temporal evolution for the near-future (2026-2050), mid-  
385 century (2051-2075) and end-century (2076-2100). The purpose of subdividing the analysis into three  
386 time periods was to compare whether, or to what extent, flood and drought characteristics increase or  
387 decrease for different future time periods as compared to a historical period.

388 In this study, we characterized floods in terms of four indices consisting of flood peak, flood volume,  
389 duration, and flashiness (Fig. 2c). The 2-year flood streamflow was used as a threshold for defining  
390 flood events, as it has been often used as a substitute of the threshold for bankfull discharge in previous  
391 studies (Cheng et al., 2013; Wu et al., 2020; Xu et al., 2019). Daily streamflows that were greater than  
392 the 2-year flood threshold were considered as flood flows. Flood flows occurring on multiple  
393 consecutive days were considered as a single flood event. The flood indices, i.e., flood peak, volume,  
394 duration, and flashiness were derived with respect to event hydrographs. Flood volume is the cumulative  
395 flow from the initial to the end of a flood event with respect to the 2-year flood streamflow level, and  
396 represents the flood intensity for different flood events (Wang et al., 2015). The annual total flood  
397 volume is the total amount of water associated with all flood events during a water year. We calculated  
398 the annual total flood volume based on flood duration and the average amount of streamflow per event  
399 in a water year. Flood duration varies for different floods and is, therefore, an important characteristic  
400 of a flood event. We summed the flood duration of each event in a water year to obtain the annual flood  
401 days. In addition, the annual maximum peak flow was derived from the daily flows to investigate  
402 changes in the characteristics of extreme floods. We extracted the 2-year flood threshold for a  
403 hydrological station based on the streamflow-exceedance probability curve. Flashiness is a measure of  
404 flood severity and is defined as the difference between the peak discharge and action stage discharge  
405 normalized by the flooding rise time (Saharia et al., 2017).

406 We characterized hydrological drought characteristics using four indices consisting of the number of  
407 droughts, annual drought days, drought duration and deficit (Fig. 2d). A threshold method was used to  
408 define hydrological drought events because it can determine the start and end of a hydrological drought  
409 event, which allows further assessment of drought characteristics, such as frequency, duration, and

410 intensity of a drought event (Cammalleri et al., 2017). It is based on defining a flow threshold (discharge,  
 411  $Q$ , m<sup>3</sup>/s), below which a hydrological drought event is considered to occur (also known as a low flow  
 412 spell). A daily variable threshold, defined as an exceedance probability of the 365 daily flow duration  
 413 curves was used to derive drought events from daily streamflow records (Fleig et al., 2006; Hisdal and  
 414 Tallaksen, 2003). For rivers with perennial flow, relatively low streamflows ranging from  $Q_{70}$  to  $Q_{95}$   
 415 have been used as a reasonable threshold (Tallaksen and van Lanen, 2004; Zelenhasić and Salvai, 1987).  
 416 In this study, we chose the 90th percentile ( $Q_{90-n}$ ) streamflow as the daily threshold, which also used as  
 417 the threshold for identifying droughts in future climate change scenarios. The  $Q_{90-n}$  of all days was  
 418 determined based on the observed historical daily streamflow.

419 To enable the comparison across different modeling scenarios (i.e., historical scenarios and future  
 420 climate change scenarios), we derived drought days, deficit, duration, and number from identified  
 421 hydrological drought events to characterize their patterns. Drought volume deficit was calculated by  
 422 subtracting daily streamflow from the threshold level ( $Q_{90-n}$ ) during a drought event, and it presents the  
 423 severity of the drought compared to the normal streamflow conditions. Drought duration was the  
 424 cumulative number of days during a drought event, i.e., the number of days from the beginning to the  
 425 end of the drought. Annual drought days were then the cumulative drought duration in a year. The  
 426 number of droughts is expressed by the number of drought events during a study period. In addition, the  
 427 annual minimum flows of each water year were extracted and used to determine the model's ability to  
 428 simulate very low flows. The drought volume deficit was calculated as:

$$429 \quad D_k = \sum_{t_i}^{t_j} (Q_{90,t} - Q_n) \cdot 60 \cdot 60 \cdot 24 \quad (4)$$

430 where  $D_k$  is the drought volume deficit (m<sup>3</sup>) of a drought event  $k$  at a hydrological station and  $t_{k,i}$  and  $t_{k,j}$   
 431 are the initial and final time steps of the run, respectively.  $Q_n$  is the daily streamflow of  $n$  day of the year  
 432 (1-365). The corresponding drought duration is computed as  $t_j - t_i + 1$ .

433 For hydrological drought events that occur relatively close in time, the inter-event time method  
 434 introduced by (Zelenhasić and Salvai, 1987) was used to separate events. This method defines a  
 435 minimum gap period,  $t_c$ , and assumes that if the inter-event time  $(t_j - t_i + 1) < t_c$ , then the consecutive events

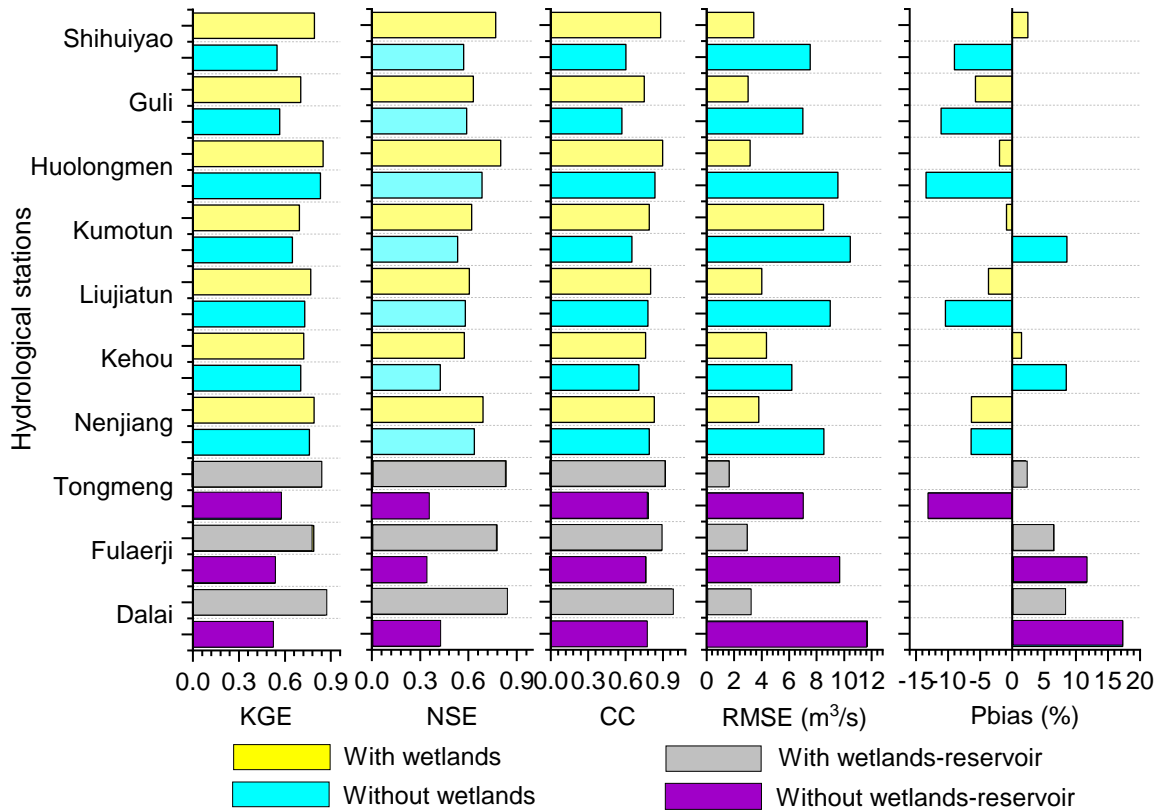
436 are interdependent and merged. In this case, the total drought deficit volume is the sum of the individual  
437 deficit values, and the event duration is the so-called real drought duration (sum of the single event  
438 duration, excluding excess periods). For this study,  $t_c$  was set equal to 7 days as recommended by  
439 (Cammalleri et al., 2017).

440

### 441 **3. Results**

#### 442 3.1 Model performance on daily streamflow and hydrography

443 Fig. 3 depicts model performances for calibration results in the presence or absence of the wetlands  
444 and the combination of wetlands and reservoir at the ten hydrological stations in the NRB. In the case  
445 of whether the wetlands were present or absent, the simulated daily streamflow results all achieved the  
446 acceptable performance criteria ( $NSE > 0.5$  and  $Pbias \leq \pm 15\%$ ) suggested by (Moriiasi, 2007) and  
447 (Moriiasi et al., 2015) at the Shihuiyao, Guli, Huolengmen, Kumotun, Kehou, Liujiatun and Kumotun  
448 stations. However, compared with the calibrated results of the model without wetlands, the simulation  
449 efficiency under with wetland scenario improved to varying degrees. Specifically, the relative  
450 improvement (i.e., the relative change) of KGE values at Shihuiyao, Guli, Huolengmen, Kumotun,  
451 Kehou, Liujiatun, Kumotun, Tongmeng, Fulaerji and Dalai were 44%, 24%, 2%, 6%, 5%, 3%, 4%, 46%,  
452 47% and 67%, respectively. In addition, the NSE and CC values were generally larger in the presence  
453 of wetlands than those in the absence of wetlands, and the RMSE and Pbias values are generally smaller  
454 than those in the absence of wetlands, showing that integrating wetlands into the hydrological model  
455 can slightly improve the model calibration results.



456

457

Figure 3. Model performances for calibration results for the with/without wetlands and reservoir

458

scenarios at the ten hydrological stations in the Nenjiang River Basin. The KGE, NSE, CC, KGE,

459

RMSE and Pbias refer to Kling-Gupta efficiency, Nash-Sutcliffe efficiency, Correlation Coefficient,

460

Root Mean Square Error, and the percentage bias, respectively.

461

462

For the lower reaches of Nierji Reservoir (i.e., the Tongmeng, Fulaerji and Dalai stations, representing

463

inclusion of the wetlands and the reservoir operation into hydrological modeling), the NSE and CC

464

values were greatly higher and RMSE and Pbias values were substantially lower when the wetlands and

465

reservoir were considered, in comparison to the case without wetlands-reservoir (Fig. 3). In fact, in the

466

scenario without wetlands-reservoir, the simulated daily streamflow results failed the acceptable

467

performance criteria ( $NSE > 0.5$  and  $Pbias \leq \pm 15\%$  as suggested by Moriasi (2007) and Moriasi et al.

468

(2015). In addition, the simulated daily streamflow in the no-wetland and no wetlands-reservoir

469

scenarios both overestimated the high flows, especially those during the flood periods; during the low

470

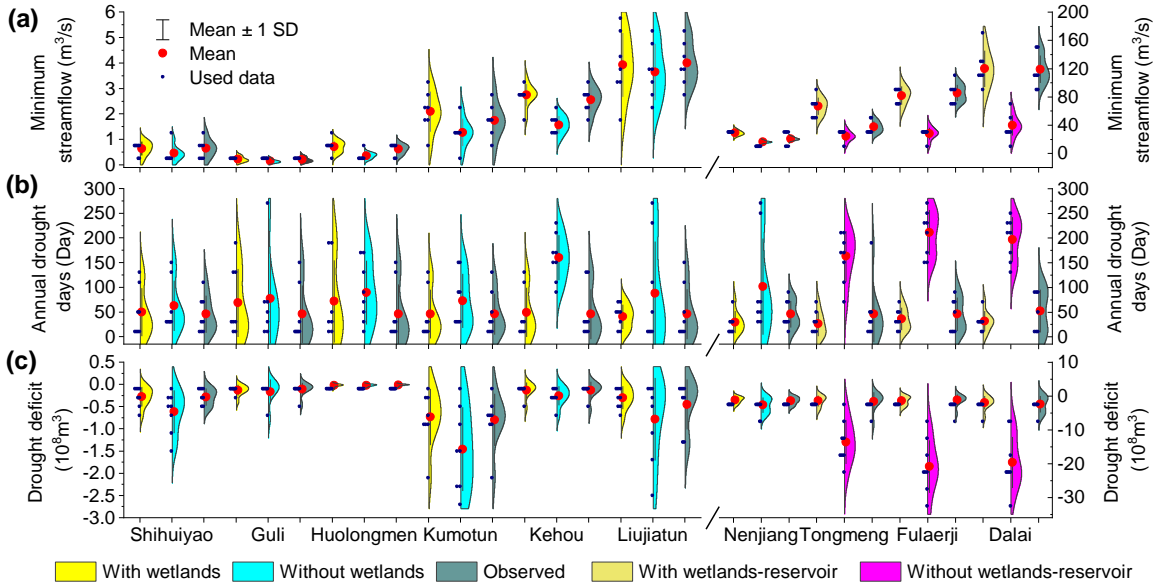
flow periods, the low flows were underestimated (Please refer to Fig. S1 in Supplementary materials).

471 Further, the simulated hydrographs under the wetland and wetlands-reservoir scenario were in much  
472 better agreement with the hydrographs of observed streamflow, especially during floods and the low-  
473 flow period (Please refer to Fig. S2 in Supplementary materials). These results indicate that inclusion  
474 of the wetlands and the operation of reservoirs can greatly improve model capacity to replicate basic  
475 hydrograph characteristics and capture hydrological extremes (e.g., high and low flows).

### 476 3.2 Model capacity to replicate flood and drought characteristics

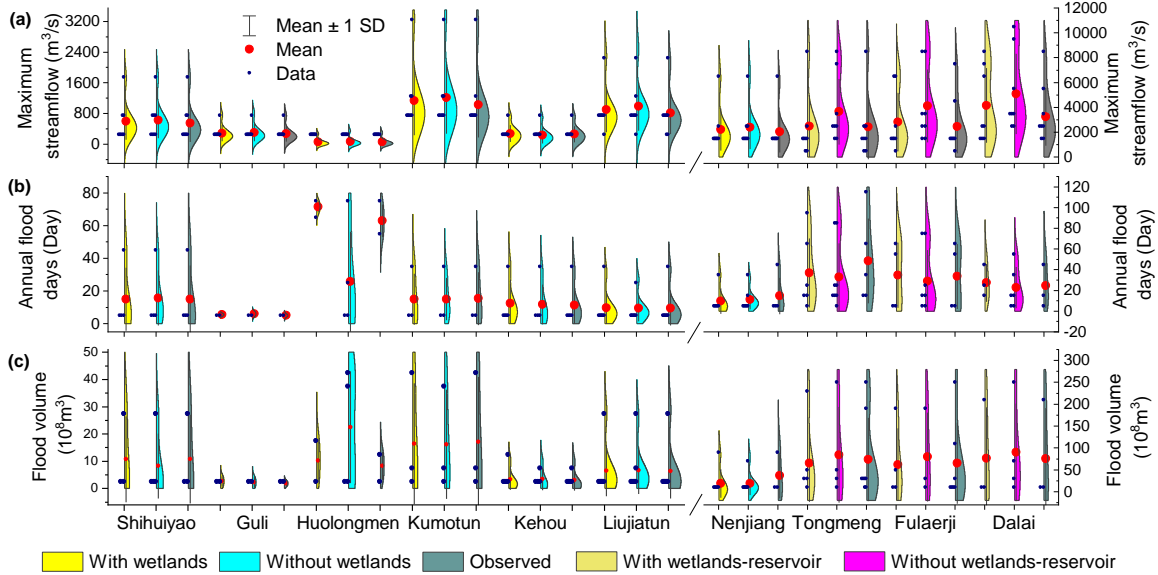
477 The simulated annual minimum streamflow for the wetlands/wetlands-reservoir scenarios were, in  
478 general, slightly overestimated or approximately equivalent to the observations compared to the  
479 scenarios that did not include the wetlands/wetlands-reservoir (Fig. 4 and Fig. 5). However, the  
480 simulation results without wetlands clearly underestimated minimum streamflow, distinctly  
481 overestimated annual drought days and drought deficit compared to the simulation results for the  
482 scenario with wetlands at the ten hydrological stations (Fig. 4). In addition, the simulated annual  
483 maximum peak flow, flood days and volume under the with/without wetland scenarios are, in general,  
484 approximately comparable to observations at the Guli, Kumotun, Kehou, Liujiatun and Nenjiang  
485 hydrological stations (Fig. S4). Specifically, for the upstream Nierji Reservoir, it is apparent that if  
486 wetlands are not considered, the number of annual flood days will be overestimated, whereas flood  
487 volume will be substantially underestimate at the Huoloengmen Station. For the lower reach of Nierji  
488 Reservoir, lack of integrating the wetlands and reservoir into the simulation can lead to a notable  
489 underestimation of annual flood days, and a substantial overestimation of the annual maximum peak  
490 flow and flood volume (Fig. 5). These results demonstrate that integrating wetlands and the combination  
491 of wetlands and the reservoir into the model can help improve model performance with regards to flow  
492 during the calibration process, and enhances the model's capability of depicting streamflow processes  
493 as well as capturing flood and drought characteristics.

494



495

496 Figure. 4. Annual minimum streamflow, drought days and deficit derived from observed records and  
 497 simulated streamflow at ten hydrological stations in the Nenjiang River Basin. The with and without  
 498 wetlands/wetlands-reservoir refers to streamflow simulation based on the presence or absence of  
 499 wetlands/wetlands-reservoir.



500

501 Figure. 5. Annual maximum peak flow, flood days and volume derived from observed records and simulated  
 502 streamflow at ten hydrological stations in the Nenjiang River Basin. The with and without wetlands/  
 503 wetlands-reservoir refers to streamflow simulation based on the presence or absence of wetlands/  
 504 wetlands-reservoir.

504

### 505 3.3 Projection of future floods

506

507 A comparison between historical and projected flood characteristics at the Nenjiang Station  
 508 (representing inclusion of wetlands into hydrological modeling) shows an overall increase in flood risks  
 509 in the upper NRB. The flood duration, peak flow, volume and flashiness generally exhibit larger  
 510 fluctuations in most of the scenarios (different SSPs and three periods as shown in Fig. S3 and Table  
 511 S1). In addition, the averaged increase in flood duration, peak flow, volume and flashiness ranges from  
 512 0.9 to 1.2%, from 16 to 33%, from 8 to 111% and from 26 to 55%, respectively (Fig.6). Specifically,  
 513 the extreme values of flood duration are much larger during the near future and end-century under the  
 514 SSP126 scenario, the end-century under the SSP370 scenario and the mid- and end-century under the  
 515 SSP585 scenario (Fig. 6a). Apart from a slight decrease during the near future and mid-century under  
 516 the SSP585 scenario, peak flow will increase through time in the SSP126, SSP370 and SSP585 scenarios  
 517 (Fig. 6b). Simultaneously, the flood volume will experience the greatest increase of 68% during the near  
 518 future under the SSP585 scenario, followed by a 22% increase during the mid-century under the SSP126  
 scenario (Fig. 6c). In terms of flashiness, the floods will be more severe under the constrains inherent

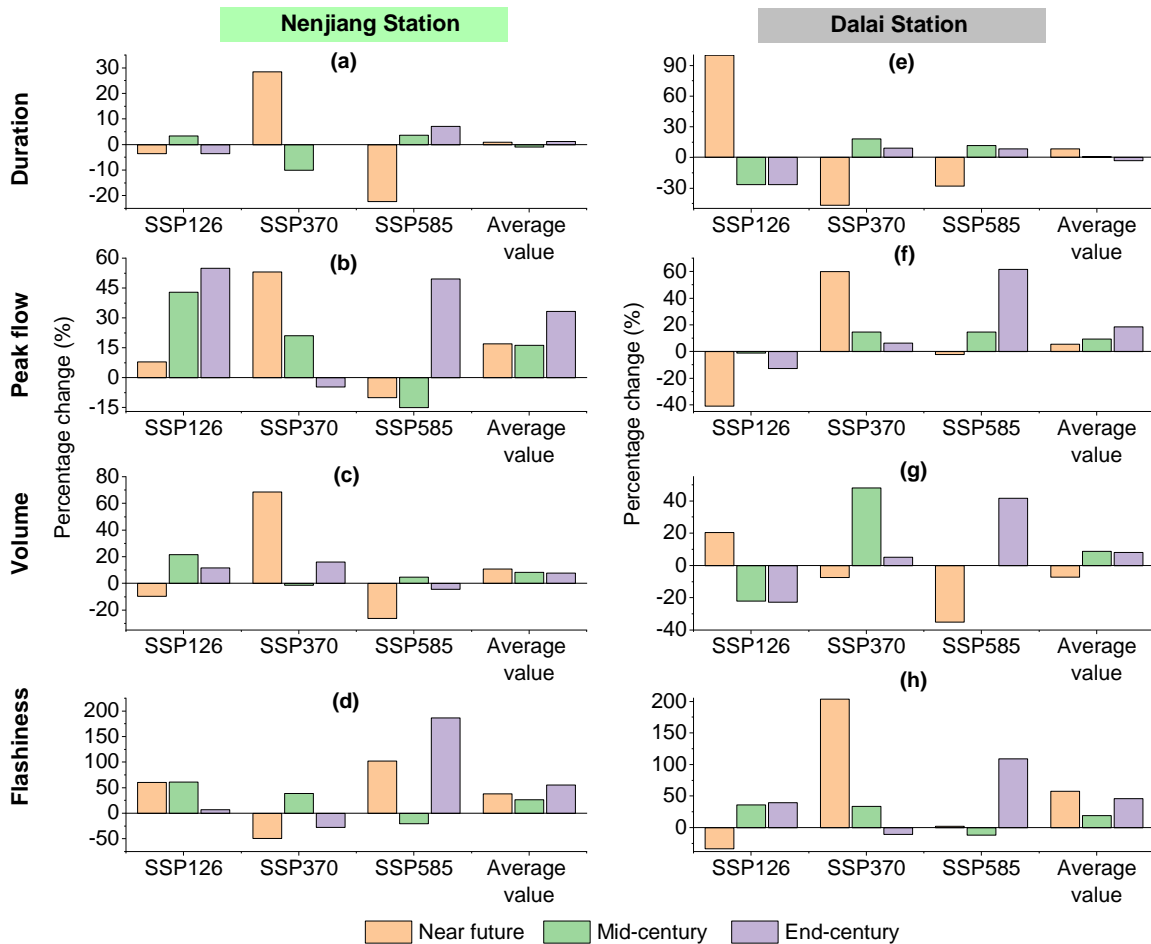
519 in the SSP126 and SSP585 scenarios and less severe given the conditions in the SSP370 scenario, as  
520 compared to the historical period (Fig. 6d).

521 It should be noted that the flood duration, peak flow, volume and flashiness can decrease in the future,  
522 as compared to the historical period (Fig.6). For example, flood duration will slightly decrease during  
523 the near future and end-century under the SSP126 scenario, largely decrease during the near future under  
524 the SSP585 scenario, respectively. Under the SSP585 scenario, the flood peak flow will experience a  
525 decrease with the percentage change values of 15% during the mid-century and the volume will reduce  
526 26% during near future. In addition, future flood flashiness will be reduced by 49% and 28% in the near  
527 future and the end-century under the SSP370 scenario respectively, and by 21% at mid-century under  
528 the SSP585 scenario.

529 The changes in the historical and future flood duration, peak flow, volume and flashiness at the Dalai  
530 Station (representing inclusion of downstream wetlands and reservoir operation into hydrological  
531 modeling) is shown in Fig.S3 and Fig.4 e-h. Similar to the Nenjiang station, the flood duration, peak  
532 flow, volume and flashiness at the Dalai station also exhibit divergent change trends across different  
533 SSPs and three periods, as compared to the historical periods. Flood duration is projected to increase  
534 largely in the near-future period for the SSP126 scenario, both in the mid-century and end-century for  
535 the SSP370 scenario (Fig.6e). The peak flow will broadly decrease for the SSP126 scenario, and increase  
536 for the SSP370 and 585 scenarios (Fig.6f). Flood volume shows divergent change trends under the three  
537 SSPs (Fig.4g). For the SSP126 scenario, flood volume will grow in the near-future and diminish in the  
538 mid- and end-century. Flood volume will decrease in the near-future, increase in the mid-century, and  
539 increase slightly in the end-century under the SSP370 scenario. However, following an apparent  
540 reduction in the near-future, flood volume is anticipated to have no discernible change trend in the mid-  
541 century and a clear increasing trend in the end-century for the SSP585 scenarios. Flashiness will be  
542 reduced in the near future and will increase in the mid-century and end-century for the SSP126 scenario  
543 (Fig.6h). For the SSP370 scenario, flashiness will increase substantially with percentage changes of 204%  
544 in the near-future, Moreover, for the SSP585 scenario, flashiness will experience a considerable increase  
545 with percentage changes of 109% in the end-century respectively. In terms of the averaged percentage



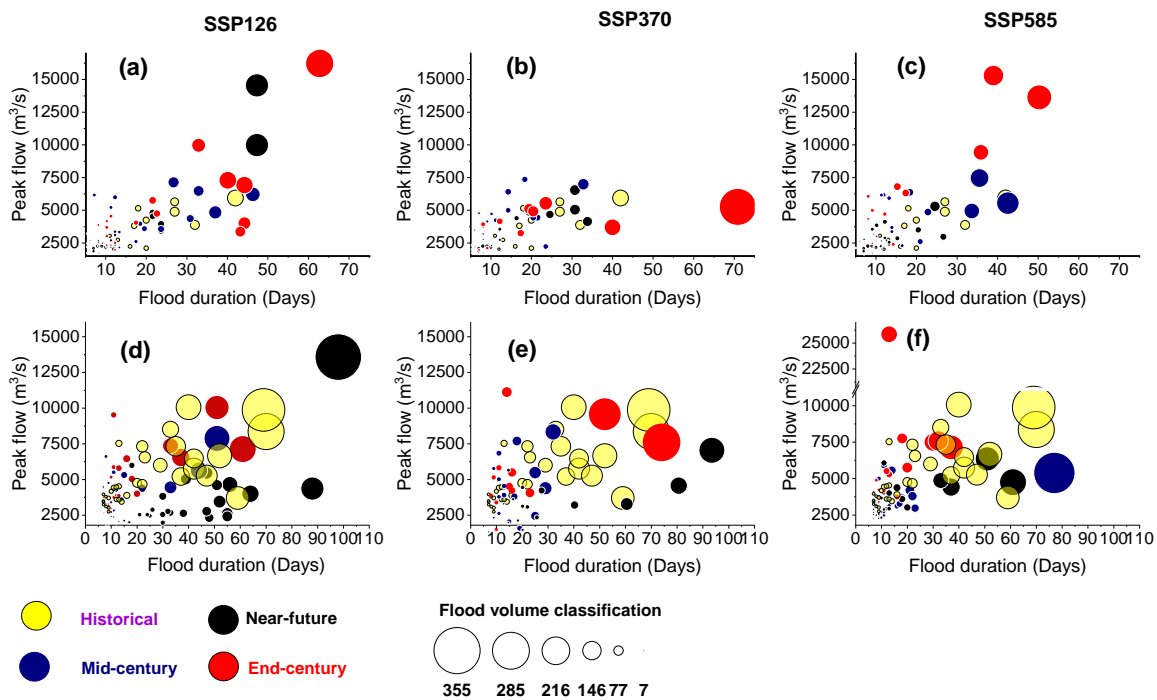
546 change values, the peak flow and flood flashiness will overall increase; the flood volume will reduce in  
 547 the near future and rise in the mid-century and end-century; and flood duration will experience a slight  
 548 increase to a minor decrease.  
 549



550  
 551 Figure 6. Projected percentage changes (relative to historical period during 1971-2020) in flood duration,  
 552 peak flow, volume and flashiness at the Nenjiang (the left column) and Dalai (the right column) Station. The  
 553 near-future, mid-century and end-century refer to the 2026-2050, 2051-2075 and 2076-2100 under the  
 554 Socioeconomic Pathways (SSP) 126, SSP370 and SSP585 scenarios. The average values were calculated  
 555 based on the projected percentage changes in the three SSP scenarios.  
 556

557 To further investigate flood risks in the NRB under future climate change, the flood duration-peak  
 558 flow-flow volume relationships at the Nenjiang and Dalai stations for the SSPs were compared to those

559 of the historical period and analyzed (Fig. 7a-c). Compared with historical flood risk, extreme flood  
 560 events with longer and larger volumes will occur more frequently at the Nenjiang Station for the SSP126  
 561 and SSP585 scenarios (Fig. 7a and 7c). It is noteworthy that the flood peak-volume-duration  
 562 relationships between the historical period and SSP370 scenario are approximate equal, with the  
 563 exception that longer duration and larger volume floods will occur during the end-century period (Fig.  
 564 5b). In addition, extreme flood events will occur mainly in the near-future for the SSP126 scenario and  
 565 during the mid- and end-century for the SSP585 scenario. Moreover, for the SSP370 and SSP585  
 566 scenarios, floods will become shorter in duration, and possess a lower peak flow and flood volume in  
 567 the near-future. Thus, the upper NRB will experience more severe flood events to a large extent under  
 568 most future climate change scenarios.  
 569



570  
 571 Figure 7. Historical and projected flood duration-peak flow-volume relationships at the Nenjiang (the  
 572 first row) and Dalai (the second row) Station. The historical period refers to 1971-2020 and the near-  
 573 future, mid-century and end-century refer to the 2026-2050, 2051-2075 and 2076-2100 under the  
 574 Socioeconomic Pathways (SSP) 126 (the first column), SSP370 (the second column) and SSP585 (the

575 third column) scenarios.

576

577 The duration-peak flow-volume relationships of extreme flood events under future climate change  
578 scenarios are closer to those of the historical period at the Dalai Station than at the Nenjiang Station  
579 (Fig. 7d-f). For the three future SSPs, the flood events with longer duration, higher peak flows or larger  
580 volume than the historical period will occurred infrequently, and the duration, flood volume and peak  
581 flow of the other shorter and lower magnitude flood events will generally be attenuated. However, very  
582 extreme flood events are projected to occur in the near-future under the conditions of scenario SSP126  
583 (Fig. 7d). Likewise, future climate change under the SSP370 scenario and 585 scenarios are projected  
584 to result in longer flood events in the near-future and mid-century, respectively (Fig. 7e and 7f).  
585 Therefore, the future flood risk can be effectively attenuated to a great extent by the combined influence  
586 of wetlands and reservoir. However, extreme floods will still occur in the future.

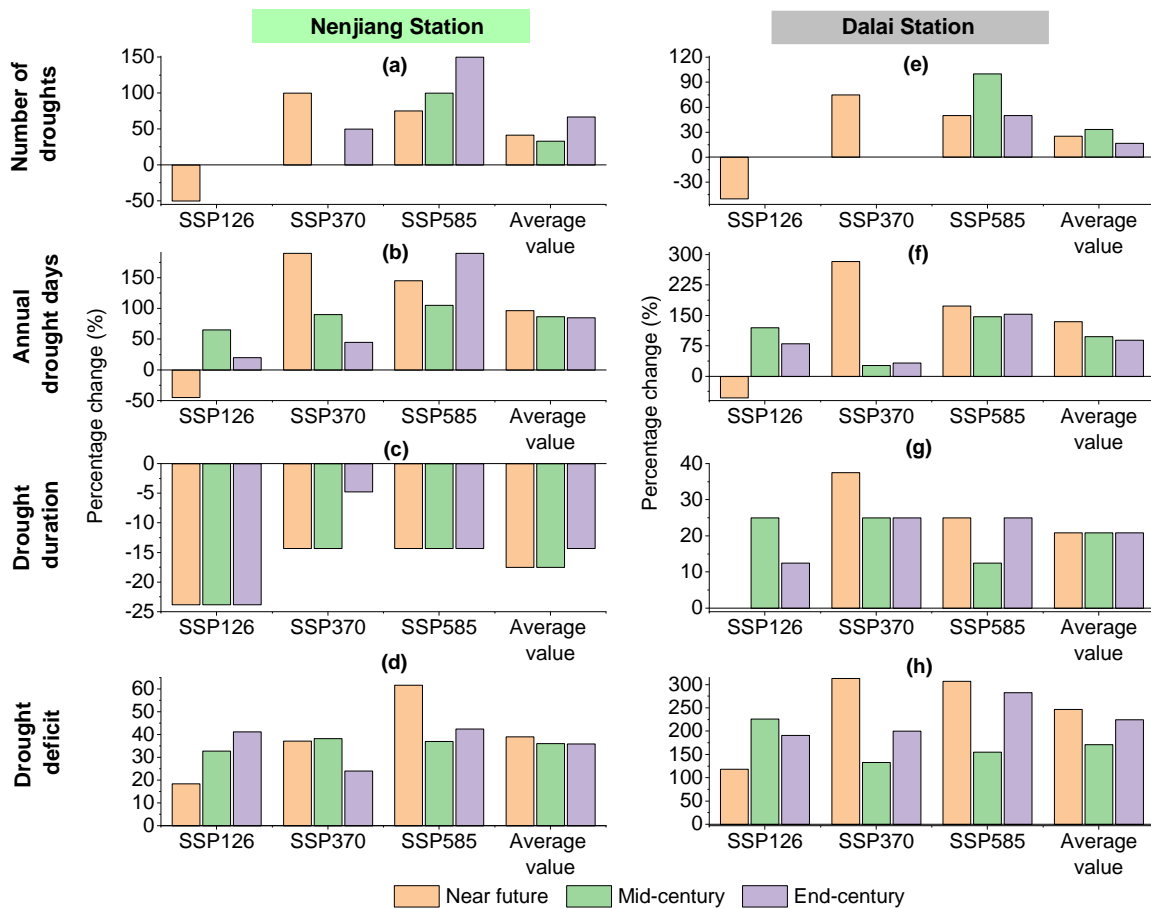
#### 587 3.4. Prediction of future hydrological droughts

588 The comparison between historical and projected hydrological drought indices shows that the risks  
589 of hydrological droughts will be increased to some extent under future climate change for both Nenjiang  
590 and Dalai stations. Specifically, in addition to a reduction in the number of droughts and annual drought  
591 days in the near future for the SSP126 scenario, the number of droughts (Fig. 8a and 8e), annual drought  
592 days (Fig. 8b and 8f) and drought deficit (Fig. 8d and 8h) will overall increase in other periods for three  
593 scenarios (Figure S4 and Table S2). It is clear that the number of droughts will be equivalent to the  
594 historical period in the mid-century and end-century for the SSP126 scenario and in the mid-century for  
595 the SSP585 scenario. For all other scenarios, the number of droughts will increase. In terms of the mean  
596 percentage change values, there is a general trend towards an increase in the number of droughts and  
597 annual drought days, which indicate that future drought events will be more frequent and there will be  
598 more days per year affected by drought. The predicted extreme values show that the future duration of  
599 drought at Nengjiang station may shorter than the historical period, but the degree of shortening  
600 presented in different SSP scenarios varies (Fig. 8c and 8g). For the Dalai station, the longest drought  
601 durations would all exceed historical extremes in the end-century for the SSP126 and SSP585 scenario,

602 and in the near future for the SSP370 scenario. The percentage change values display that drought  
 603 duration will be reduced at the Nenjiang station and will be extended at the Dalai station for all the SSP  
 604 scenarios. Drought deficit at the Dalai station will increase by 39%, 36% and 36% and in the near future,  
 605 mid-century and end-century. For the Dalai station, drought deficit will increase further in the three  
 606 periods with 39%, 36% and 36%, respectively.

607 A comparison of the percentage change values between the Nenjiang and Dalai stations shows that,  
 608 apart from a reduction of the number of drought events, the risk of drought to be experienced at Dalai  
 609 is considerably stronger than at Nenjiang. Specifically, the percentage change in the annual drought  
 610 days, drought duration and deficit will increase from 85-97% to 89-134%, from -17- -17% to 21%, and  
 611 from 36-39% to 171-247%, respectively.

612



613

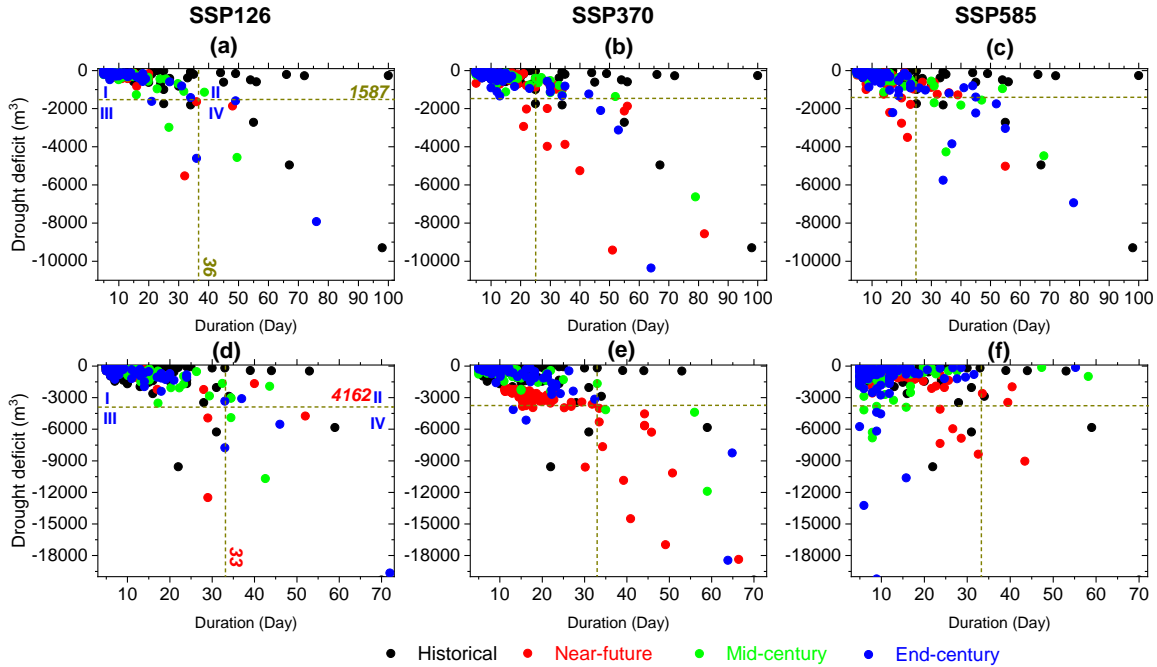
614 Figure 8. Projected percentage changes (relative to historical period during 1971-2020) in hydrological

615 drought characteristics at the Nenjiang (the left column) and Dalai (the right column) Station. The near-future,  
616 mid-century and end-century refer to the 2026-2050, 2051-2075 and 2076-2100 under the Socioeconomic  
617 Pathways (SSP) 126, SSP370 and SSP585 scenarios. The average values were calculated based on the  
618 projected percentage changes in the three SSP scenarios.

619

620 To further analyze the temporal evolution of droughts in the Nenjiang River Basin under future  
621 climate change, drought events were classified into four types in terms of duration and deficit, i.e., short-  
622 term light droughts, long-term light droughts, short-term severe droughts, and long-term severe droughts  
623 (see Fig. 9 for details). This four-part classification was then used to compare and analyze the changes  
624 in the temporal characteristics of drought events under the different SSP scenarios. Similar to the  
625 drought characteristics during the historic historical period, the majority of drought events for the  
626 SSP126, SSP370 and SSP585 scenarios are short-term light droughts (Fig. 9a-c), i.e., the upper NRB  
627 will still be dominated by short-term light droughts under future climate change. However, these  
628 droughts will be slightly aggravated and marginally longer. In addition, long-term light droughts will  
629 occur rarely under the conditions inherent in scenarios SSP126 (Fig. 9a) and SSP370 (Fig. 9b), and  
630 occur relative frequently in the SSP585 scenario (Fig. 9c). However, compared with the historical period,  
631 the overall number of long-term light droughts will largely decrease, but the deficit will increase slightly  
632 under future climate change. In addition, short-term severe droughts will increase substantially, along  
633 with their deficit. The number of long-term severe droughts for the SSP126 scenario is approximately  
634 the same as in the past, but the duration will be substantially reduced. For scenarios SSP370 and SSP585,  
635 the number of long-term severe droughts will increase more than during the historical period, but the  
636 duration will be markedly less, and the deficit will be reduced to some extent. In terms of the different  
637 the sub-periods, severe droughts in the upper NRB will be more severe during the near-future and end-  
638 century periods, and relatively less severe in the mid-century period in comparison to the historical  
639 period. However, overall, the droughts will be of shorter duration and characterized by an increased  
640 deficit under future climates.

641



642

643 Figure 9. Historical and projected duration-deficit relationship of each hydrological droughts at the Nenjiang  
 644 (the first row) and Dalai (the second row) Station. The historical period refers to 1971-2020 and the near-  
 645 future, mid-century and end-century refer to the 2026-2050, 2051-2075 and 2076-2100 under the  
 646 Socioeconomic Pathways (SSP) 126 (the first column), SSP370 (the second column) and SSP585 (the  
 647 third column). The dark yellow lines in the horizontal and vertical directions refer the 95% threshold lines  
 648 for drought deficit and duration values, respectively. I, II, III and IV refer to short-term light droughts, long-  
 649 term light droughts, short-term severe droughts, and long-term severe droughts, respectively.

650

651 Droughts brought about by future climate change at the Dalai Station located along the lower reaches  
 652 of the NRB will continue to be dominated by short-term slight droughts (Fig. 9d-f). For the SSP126  
 653 scenario, the duration and deficit of the short-term slight droughts will be approximately the same as  
 654 those during historical times (Fig. 9d). However, the duration and deficit of short-term slight droughts  
 655 will increase given the conditions specified in the SSP370 (Fig. 9e) and SSP585 (Fig. 9f) scenarios. The  
 656 duration of short-term slight droughts will increase the most for scenario SSP370. In addition, under all  
 657 three SSP scenarios, long-term slight droughts will, in general, be reduced. In fact, under the SSP370  
 658 scenario, long-term slight droughts will not occur. The number of short-term severe droughts will

659 generally tend to increase, with the most pronounced increase under the SSP585 scenario, followed by  
660 the SSP370 scenario. A slight increase will occur under the SSP126 scenario. However, long-term  
661 severe droughts will increase substantially under the SSP126 and SSP370 scenarios. In particular, under  
662 the SSP370 scenario, the duration of long-term severe droughts will be exceptionally prolonged, and  
663 the severity will be extraordinarily increased, indicating that the risk of droughts of long duration and  
664 with a severe deficit will climb abnormally in some year. For example, under the conditions set by the  
665 SSP370 scenario, the deficit of long-term severe droughts will reach -18,169 m<sup>3</sup> and -18,457 m<sup>3</sup> during  
666 the near-future and end-century periods. For the SSP585 scenario, long-term severe drought will occur  
667 only once in the near-future, which is equivalent to the historical period. These results indicate that the  
668 risk of future hydrologic droughts along the lower NRB will further increase even under the combined  
669 influence of reservoirs and wetlands.

670

#### 671 **4. Discussion**

672 4.1. Integrating wetlands and reservoir operation into basin hydrologic modeling and basin water  
673 management

674 A series of studies have shown that the simulation and prediction of floods and droughts faces many  
675 challenges, such as the scarcity of hydrometeorological driven data (Foulon et al., 2018), model errors  
676 (Golden et al., 2021; Smakhtin, 2001; Staudinger et al., 2011) and anthropogenic disturbances (e.g.,  
677 reservoir operation) (Brunner, 2021; Brunner et al., 2021). In this study, we developed a spatially  
678 explicit hydrological model that considers wetland hydrological processes and reservoir operations  
679 through coupling a distributed hydrological modeling platform with wetland modules and reservoir  
680 simulation algorithms. We found that coupling wetland alone or coupling wetlands and reservoir with  
681 hydrological model can improve model calibration results and model performance of capturing flood  
682 and drought characteristics in a large river basin. Such model performance improvement can provide  
683 important information for developing downstream water resources management. Previous studies have  
684 shown that climate change is further exacerbating the risk of hydrological extremes, leading to an

685 expanding of flood and drought affected area (Diffenbaugh et al., 2015; e.g., Hirabayashi et al., 2013;  
686 Wang et al., 2021), which increase the complexity of accurate prediction and the challenge for effective  
687 mitigation. Give that, projecting flood and drought risks in response to a changing climate requires  
688 robust hydrologic models that take into account the important factors within a watershed that can largely  
689 influence basin hydrological processes (Golden et al., 2021). Therefore, in basins that coexist with high-  
690 coverage wetlands and multiple reservoirs, it is necessary to integrate wetlands and reservoir operation  
691 into basin hydrological simulation, thus providing practical support for extreme hydrological risk  
692 mitigation and water resource management under a changing climate.

693 Although our developed framework demonstrates good modeling results, uncertainties could exist in  
694 the assessment. Aspects such as the accuracy and error of the input data (Lobligeois et al., 2014), the  
695 choice of the objective function (Fowler et al., 2018), the length of the period considered during  
696 calibration (Arsenault et al., 2018), and the model structure (Melsen et al., 2019) can all affect the  
697 performance of a model to replicate streamflow, thus impacting flood and drought predictions and water  
698 management under future climate change. In addition, due to a lack of wetlands water balance  
699 monitoring data, this study only used river station data (which only considered the cumulative  
700 hydrologic effect of upstream wetlands) for model calibration. Therefore, there are ongoing efforts to  
701 obtain sufficient observations on wetland area dynamics and evapotranspiration, water depth and  
702 volume, soil water content and actual observations to better calibrate/validate watershed hydrological  
703 models, which are expected to better provide key parameters for further improving the model's capacity  
704 to capture flood and drought patterns and better serve basin water management. In addition, the several  
705 SPPs employed to drive the simulation framework, including SSP126, SSP370, and SSP585 scenarios,  
706 can introduce uncertainty into future flood and drought risk projections. Because of the internal  
707 variability and uncertainties inherent in the existing climate models (Qing et al., 2020; Martel et al.,  
708 2022), the projection findings under different scenarios were inconsistent, creating a challenge for pro-  
709 active management and mitigation decisions. Despite the climate models' recognized flaws and  
710 uncertainties, the general concordance between models and observations over many regions suggests  
711 some improved confidence in their utility for understanding and mitigating future drought and climate



712 change (Cook et al., 2020). Furthermore, several reservoirs and a large number of wetlands are spread  
713 throughout the NRB's tributaries (Meng et al., 2019), which individually and together play an essential  
714 role in drought and flood risk reduction. We only investigated the impacts of mainstream reservoirs and  
715 wetlands on drought and flood risk due to a lack of sub-basin reservoir operation observations. As a  
716 result, future integrated wetland-reservoir simulations of all mainstream and tributaries for flood-  
717 drought risk assessment will be done based on further data collection. Since the Nierji reservoir is the  
718 largest in the NRB and has the most influence on the mainstream runoff regime, our findings based on  
719 the simulation of Nierji reservoir and wetlands can give new insights into future floods and droughts, as  
720 well as provide important support for future hydrological extremes adaptation.

#### 721 4.2. The combining mitigation efficiency of wetlands and reservoir operation

722 The relative changes (compared with historical periods) of future flood and drought indices (Fig. 6  
723 and 8), duration-peak flow-volume relationships (Fig. 7) and duration-deficit relationship (Fig. 9) differ  
724 between the Nenjiang and Dalai stations under the same SSP scenario or in the same period, indicating  
725 that reservoirs and downstream wetlands can modify the continuous propagation of upstream flood and  
726 hydrological drought risks to the downstream. First, reservoirs and downstream wetlands can help to  
727 reduce the risks of future floods and droughts to some extent, namely partially reduce flood peak flow  
728 and flashiness, and decrease the number of droughts, annual drought days and drought deficit. Second,  
729 reservoirs and downstream wetlands cannot completely eliminate flood and drought risks. Because the  
730 flood duration and volume will overall increase at the Dalai station, especially that the extreme floods  
731 will be more frequent in the future (Fig.7). Further, in addition to the number of droughts, the percentage  
732 change values of the annual drought days, drought duration and deficit relative change at the Dalai  
733 Station are greater than those of Nenjiang Station (Fig.8). This imply that the mitigation effects on  
734 hydrological droughts is minimal. Such findings suggest that future climate change will lead to an  
735 increase in the risk of hydrologic failure of existing reservoir and wetlands, thus posing large challenges  
736 for future socio-and eco-hydrological systems in the downstream NRB.

737 Wetlands are typically viewed as green infrastructures and reservoirs are generally regarded as  
738 important gray infrastructures. Although our study showed that the combining of reservoirs and

739 wetlands does not completely eliminate the risk of future hydrological extremes, they continue to play  
740 an important role that cannot be ignored. The reservoir's inherent constraints are one factor contributing  
741 to this likelihood of hydrological failure. This is because reservoirs only control floods and droughts  
742 that occur downstream of them, limiting their effects to the regional scale (Brunner, 2021). The  
743 regulation becomes less effective with distance increased due to "dilutions" effect caused by inflows  
744 from downstream tributaries (Guo et al., 2012). Reservoirs cannot, however, play a considerable role in  
745 basins where tributaries exist downstream, particularly those sub-basins prone to drought and flooding.  
746 From these perspectives, widely distributed wetlands can provide a complementary and vital function  
747 by providing biological function and hydrological regulation in regions where reservoirs are unable to  
748 have an impact. On the other hand, the limited capacity of existing wetlands to regulate hydrology  
749 increases the risk of hydrological failure to some extent. This is because, compared with the historical  
750 period, the existing wetlands in the NRB have been seriously degraded, such as the weakening of the  
751 connectivity between riparian wetlands and the river channel, and the increased fragmentation of  
752 wetlands, among other changes (Chen et al., 2021). These degraded wetlands cannot play an effective  
753 role in mitigating floods and droughts under future climate change.

754

#### 755 4.3. Implications for flood and drought risk management under climate change

756 This modeling study predicts higher flood and drought risks in the NRB under the combined influence  
757 of wetlands and reservoirs. This could impose a great challenge to the operation of the Nierji Reservoir  
758 dam, i.e., to its effective operation for flood mitigation and drought alleviation. To curb the flood and  
759 drought risks caused by future climate change in the NRB, it is urgent to improve the water regulation  
760 capacity of the lower NRB. Although the Nierji Reservoir, as previously argued, plays an important role  
761 in reducing floods and droughts, the potential for extreme hydrological events in the future necessitate  
762 the application of various combinations of measures with different scales of implementation (i.e., hybrid  
763 measures). We insist that the first remedial measure to be undertaken should be the implementation of  
764 wetland restoration and protection projects, because studies have demonstrated that wetland coverage  
765 and their spatial pattern can affect both basin physical conditions and human decision-making attitudes

766 toward risk (Gómez-Baggethun et al., 2019; Javaheri and Babbar-Sebens, 2014; Martinez-Martinez et  
767 al., 2014; Zedler and Kercher, 2005). Given that the spatial location of wetlands within a river basin is  
768 also important in determining the efficiency of their mitigation services (Gourevitch et al., 2020; Li et  
769 al., 2021; Zhang and Song, 2014), optimization of wetland spatial patterns should be considered and can  
770 be carried out to further enhance the role of wetlands in flood and drought defense.

771 In our view, the second important remedial measure that should be implemented is to improve the  
772 existing reservoir operation schemes based on accurate hydrological forecasting. This requires, on one  
773 hand, coupling of wetlands with hydrological processes and models to improve the simulation accuracy  
774 of the upstream incoming water (i.e., runoff from the Nenjiang Station) to provide scientific support for  
775 reservoir operation decisions. Concomitantly, it is necessary to modify the existing schemes for optimal  
776 reservoir operation to improve the system's capacity to deal with extreme flood and drought risks.  
777 Because the percentage increase in flood (Fig. 6) and drought indicators (Fig. 8) demonstrated that the  
778 existing reservoir operation schemes are not effective in mitigating the risks associated with future  
779 climate change-induced floods and droughts. Therefore, we need to re-examine and evaluate the flood  
780 and drought risks in the NRB under future climate change and propose optimal operation schemes that  
781 can maximize the reduction of flood and drought risks by the Nierji Reservoir. Traditionally, the water  
782 level of a reservoir should be maintained at the designed flood limited water level during the flood  
783 season, which does not consider river flow forecast. (Ding et al., 2015) analyzed a concept that provides  
784 a dynamic control of the maximum allowed water level during the flood season, for the Nierji Reservoir  
785 dam. A reasonable approach to tackle this issue could be to considerate forecast uncertainty and  
786 acceptable flood risk to minimize the total loss caused by flood and drought. Further modeling studies  
787 with multi-objective optimization algorithm can help identify an optimum reservoir operation for best  
788 economic and ecological outcomes.

## 789 **5. Conclusions**

790 This study projected future flood and drought risks by considering the combined impacts of wetlands  
791 and reservoirs. To achieve this, we developed a hydrological modeling framework coupled wetlands

792 and reservoir operations and then applied it in a case study involving a 297,000-km<sup>2</sup> large river basin in  
793 northeast China. With this framework, we found that coupling wetlands and reservoir operations can  
794 slightly increase model calibration results and efficiently improve model capacity to capture both flood  
795 and hydrological drought characteristics in a river basin. The upper NRB will experience more severe  
796 flood and hydrological droughts and can impose a great challenge to the effective operation of  
797 downstream reservoir under the predicted future climate change scenarios. The risk of future floods and  
798 hydrologic droughts along the lower NRB will further increase even under the combined influence of  
799 reservoirs and wetlands. These results demonstrated that the risk of floods and droughts will overall  
800 increase further under future climate change even under the combined influence of reservoirs and  
801 wetlands, showing the urgency to implement wetland restoration and develop accurate forecasting  
802 systems. To fully understand how wetland and reservoir operations may be influential and maintain an  
803 acceptable level of risk, it is therefore necessary to consider an optimization of wetland spatial patterns  
804 and reservoir operations simultaneously, thus achieving a collaborative optimization management to  
805 maximum basin resilience to floods and hydrological droughts. Further, the effects of combining NBS  
806 (e.g., wetlands) with traditional engineering solutions (e.g., reservoir) should both be useful and  
807 necessary in the future for management decisions.

808

#### 809 **Data Availability**

810 The data used in this study are openly available for research purposes. The five GCM outputs (GFDL-  
811 ESM4, IPSL-CM6A-LR, MPI-ESM1-2-HR, MRI-ESM2-0, and UKESM1-0-L) used in this study are  
812 publically available and were provided by the Inter-Sectoral Impact Model Intercomparison Project  
813 (ISIMIP) (<https://esg.pik-potsdam.de/search/isimip/>). The CMhyd software is available at  
814 <https://swat.tamu.edu/software/cmhyd>. The land-use/land-cover types, soil texture, and digital elevation  
815 model for China can be downloaded from <https://www.resdc.cn/>. Data from the 88 weather stations  
816 administered by National Meteorological Information Centre of China can be download at  
817 <http://data.cma.cn>.

818

819 **Author contribution**

820 **Yanfeng Wu:** Conceptualization, Writing, Data analysis, Methodology, Software. **Jingxuan Sun:**  
821 Formal analysis, Investigation, Data analysis and Plotting. **Boting Hu:** Software, Visualization, Data  
822 analysis. **Y. Jun Xu:** Writing - review & editing. **Alain N. Rousseau:** Writing - review & editing.  
823 **Guangxin Zhang:** Conceptualization, Supervision, review & editing.

824

825 **Competing interests**

826 The authors declare that they have no known competing financial interests or personal relationships  
827 that could have appeared to influence the work reported in this paper.

828

829 **Acknowledgments**

830 We are grateful to Jan Seibert for his valuable comments on the manuscript. The authors express their  
831 gratitude to the three anonymous reviewers for their constructive comments and suggestions that have  
832 helped improve the paper. We thank Anna Feist-Polner, Lorena Grabowski, Polina Shvedko and Sarah  
833 Buchmann for their efforts in the processing of the manuscript.

834

835 **Financial support**

836 This work was supported by the National Natural Science Foundation of China (42101051), the  
837 Postdoctoral Science Foundation of China (2021M693155), the Strategic Priority Research Program of  
838 the Chinese Academy of Sciences, China (XDA28020501, XDA28020105), and The National Key  
839 Research and Development Program of China (2021YFC3200203). During preparation of this  
840 manuscript, YJX received a grant from U.S. Department of Agriculture Hatch Fund (project number,  
841 LAB94459).

842 **References**

- 843 Åhlén, I., Hambäck, P., Thorslund, J., Frampton, A., Destouni, G., Jarsjö, J.: Wetlandscape size thresholds for  
844 ecosystem service delivery: Evidence from the Norrström drainage basin, Sweden. *Sci. Total Environ.*  
845 704, 135452. <https://doi.org/10.1016/j.scitotenv.2019.135452>, 2020.
- 846 Åhlén, I., Thorslund, J., Hambäck, P., Destouni, G., Jarsjö, J.: Wetland position in the landscape: Impact on  
847 water storage and flood buffering. *Ecohydrology* 15 (7): e2458. <https://doi.org/10.1002/eco.2458>, 2022.
- 848 Alves, A., Gersonius, B., Kapelan, Z., Vojinovic, Z. and Sanchez, A.: Assessing the Co-Benefits of green-  
849 blue-grey infrastructure for sustainable urban flood risk management. *Journal of Environmental*  
850 *Management*, 239: 244-254. <https://doi.org/10.1016/j.jenvman.2019.03.036>, 2019.
- 851 Anderson, C.C. and Renaud, F.G.: A review of public acceptance of nature-based solutions: The ‘why’,  
852 ‘when’, and ‘how’ of success for disaster risk reduction measures. *Ambio*, 50(8): 1552-1573.  
853 <https://doi.org/10.1007/s13280-021-01502-4>, 2021..
- 854 Arsenaault, R., Brissette, F. and Martel, J.: The hazards of split-sample validation in hydrological model  
855 calibration. *Journal of Hydrology*, 566: 346-362. <https://doi.org/10.1016/j.jhydrol.2018.09.027>, 2018.
- 856 Beven, K.: Kinematic subsurface stormflow. *Water Resources Research*, 17(5): 1419-1424.  
857 <https://doi.org/10.1029/WR017i005p01419>, 1981.
- 858 Bosshard, T., Kotlarski, S., Ewen, T. and Schär, C.: Spectral representation of the annual cycle in the climate  
859 change signal. *Hydrology and Earth System Sciences*, 15(9): 2777-2788. [https://doi.org/10.5194/hess-](https://doi.org/10.5194/hess-15-2777-2011)  
860 [15-2777-2011](https://doi.org/10.5194/hess-15-2777-2011), 2011.
- 861 Bouda, M., Rousseau, A. N., Gumiere, S. J., Gagnon, P., Konan, B., & Moussa, R.: Implementation of an  
862 automatic calibration procedure for HYDROTEL based on prior OAT sensitivity and complementary  
863 identifiability analysis. *Hydrological Processes*, 28(12): 3947-3961. <https://doi.org/10.1002/hyp.988>,  
864 2014.
- 865 Bouda, M., Rousseau, A.N., Konan, B., Gagnon, P. and Gumiere, S.J.: Bayesian Uncertainty Analysis of the  
866 Distributed Hydrological Model HYDROTEL. *Journal of Hydrologic Engineering*, 17(9): 1021-1032.  
867 [https://doi.org/10.1061/\(ASCE\)HE.1943-5584.00005](https://doi.org/10.1061/(ASCE)HE.1943-5584.00005), 2012.
- 868 Boulange, J., Hanasaki, N., Yamazaki, D. and Pokhrel, Y.: Role of dams in reducing global flood exposure  
869 under climate change. *Nature Communications*, 12(1), 417. <https://doi.org/10.1038/s41467-020-20704->

870 0, 2021.

871 Brunner, M.I.: Reservoir regulation affects droughts and floods at local and regional scales. *Environmental*  
872 *Research Letters*, 16(12): 124016. <https://doi.org/10.1088/1748-9326/ac36f6>, 2021.

873 Brunner, M.I., Slater, L., Tallaksen, L.M. and Clark, M.: Challenges in modeling and predicting floods and  
874 droughts: A review. *WIREs Water*, 8(3). <https://doi.org/10.1002/wat2.1520>,2021.

875 Cammalleri, C., Vogt, J. and Salamon, P.: Development of an operational low-flow index for hydrological  
876 drought monitoring over Europe. *Hydrological sciences journal*, 62(3): 346-358.  
877 <https://doi.org/10.1080/02626667.2016.1240869>, 2017.

878 Casal-Campos, A., Fu, G., Butler, D. and Moore, A.: An Integrated Environmental Assessment of Green and  
879 Gray Infrastructure Strategies for Robust Decision Making. *Environmental Science & Technology*,  
880 49(14): 8307-8314. <https://doi.org/10.1021/es506144f>, 2015.

881 Chen, L., Wu, Y., Xu, Y.J. and Guangxin, Z.: Alteration of flood pulses by damming the Nenjiang River,  
882 China - Implication for the need to identify a hydrograph-based inundation threshold for protecting  
883 floodplain wetlands. *Ecological Indicators*, 124: 107406. <https://doi.org/10.1016/j.ecolind.2021.107406>,  
884 2021.

885 Cheng, C., Brabec, E., Yang, Y. and Ryan, R. Rethinking stormwater management in a changing world:  
886 Effects of detention for flooding hazard mitigation under climate change scenarios in the Charles River  
887 Watershed, Proceedings of 2013 CELA Conference, Austin, Texas, pp. 27-30, 2013..

888 Chiang, F., Mazdiyasn, O. and AghaKouchak, A.: Evidence of anthropogenic impacts on global drought  
889 frequency, duration, and intensity. *Nature Communications*, 12(1), 2754. [https://doi.org/10.1038/s41467-](https://doi.org/10.1038/s41467-021-22314-w)  
890 [021-22314-w](https://doi.org/10.1038/s41467-021-22314-w), 2021.

891 Dang, T.D., Chowdhury, A.F.M.K. and Galelli, S.: On the representation of water reservoir storage and  
892 operations in large-scale hydrological models: implications on model parameterization and climate  
893 change impact assessments. *Hydrology and Earth System Sciences*, 24(1): 397-416.  
894 <https://doi.org/10.5194/hess-24-397-2020>, 2020.

895 Diffenbaugh, N.S., Swain, D.L. and Touma, D.: Anthropogenic warming has increased drought risk in  
896 California. *Proceedings of the National Academy of Sciences*, 112(13): 3931-3936.  
897 <https://doi.org/10.1073/pnas.1422385112>, 2015.

898 Ding, W. et al., 2015. An analytical framework for flood water conservation considering forecast uncertainty  
899 and acceptable risk. *Water Resources Research*, 51(6): 4702-4726.  
900 <https://doi.org/10.1002/2015WR017127>, 2015.

901 Dobson, B., Wagener, T. and Pianosi, F.: An argument-driven classification and comparison of reservoir  
902 operation optimization methods. *Advances in Water Resources*, 128: 74-86, 2019.

903 Eriyagama, N., Smakhtin, V. and Udamulla, L.: How much artificial surface storage is acceptable in a river  
904 basin and where should it be located: A review. *Earth-Science Reviews*, 208: 103294, 2020.

905 Evenson, G.R., Jones, C.N., Mclaughlin, D.L., Golden, H.E., Lane, C.R., Devries, B., Alexander, L.C., Lang,  
906 M.W., Mccarty, G.W.Sharifi, A.: A watershed-scale model for depressionnal wetland-rich landscapes. *J.*  
907 *Hydrol. X* 1, 100002. <https://doi.org/https://doi.org/10.1016/j.hydroa.2018.10.002,2018>.

908 Evenson, G.R., Golden, H.E., Lane, C.R.D Amico, E.: Geographically isolated wetlands and watershed  
909 hydrology: A modified model analysis. *J. Hydrol.* 529, 240-256.  
910 <https://doi.org/10.1016/j.jhydrol.2015.07.039,2015>.

911 Evenson, G.R., Golden, H.E., Lane, C.R.D'Amico, E.: An improved representation of geographically isolated  
912 wetlands in a watershed-scale hydrologic model. *Hydrol. Process.* 30 (22), 4168-4184.  
913 <https://doi.org/10.1002/hyp.10930,2016>.

914 Fleig, A. K., Tallaksen, L. M., Hisdal, H., and Demuth, S.: A global evaluation of streamflow drought  
915 characteristics, *Hydrol. Earth Syst. Sci.*, 10, 535–552, <https://doi.org/10.5194/hess-10-535-2006,2006>.

916 Fortin, J. P., Turcotte, R., Massicotte, S., Moussa, R., Fitzback, J., & Villeneuve, J. P.: Distributed watershed  
917 model compatible with remote sensing and GIS data. I: Description of model. *Journal of Hydrologic*  
918 *Engineering*, 6(2), 91-99, 2001.

919 Fossey, M., Rousseau, A.N., Bensalma, F., Savary, S.Royer, A.: Integrating isolated and riparian wetland  
920 modules in the PHYSITEL/HYDROTEL modelling platform: model performance and diagnosis. *Hydrol.*  
921 *Process.* 29 (22), 4683-4702. <https://doi.org/10.1002/hyp.10534,2015>.

922 Foulon, É., Rousseau, A.N.Gagnon, P.: Development of a methodology to assess future trends in low flows  
923 at the watershed scale using solely climate data. *J. Hydrol.* 557, 774-790.  
924 <https://doi.org/10.1016/j.jhydrol.2017.12.064,2018>.

925 Fowler, K., Peel, M., Western, A.Zhang, L.: Improved Rainfall-Runoff Calibration for Drying Climate:



926 Choice of Objective Function. *Water Resour. Res.* 54 (5), 3392-3408.  
927 <https://doi.org/10.1029/2017WR022466>,2018.

928 Garcia, F., Folton, N.Oudin, L.: Which objective function to calibrate rainfall–runoff models for low-flow  
929 index simulations? *Hydrological Sciences Journal* 62 (7), 1149-1166.  
930 <https://doi.org/10.1080/02626667.2017.1308511>,2017.

931 Golden, H.E., Lane, C.R., Rajib, A.Wu, Q.: Improving global flood and drought predictions: integrating non-  
932 floodplain wetlands into watershed hydrologic models. *Environ. Res. Lett.* 16 (9), 091002.  
933 <https://doi.org/10.1088/1748-9326/ac1fbc>,2021.

934 Gómez-Baggethun, E., Tudor, M., Doroftei, M., Covaliov, S., Năstase, A., Onără, D., Mierlă, M., Marinov,  
935 M., Doroșencu, A., Lupu, G., Teodorof, L., Tudor, I., Köhler, B., Museth, J., Aronsen, E., Ivar Johnsen,  
936 S., Ibram, O., Marin, E., Crăciun, A.Cioacă, E.: Changes in ecosystem services from wetland loss and  
937 restoration: An ecosystem assessment of the Danube Delta (1960–2010). *Ecosyst. Serv.* 39, 100965.  
938 <https://doi.org/https://doi.org/10.1016/j.ecoser.2019.100965>,2019.

939 Gourevitch, J.D., Singh, N.K., Minot, J., Raub, K.B., Rizzo, D.M., Wemple, B.C.Ricketts, T.H.: Spatial  
940 targeting of floodplain restoration to equitably mitigate flood risk. *Global Environmental Change* 61,  
941 102050. <https://doi.org/10.1016/j.gloenvcha.2020.102050>,2020.

942 Gulbin, S., Kirilenko, A.P., Kharel, G.Zhang, X.: Wetland loss impact on long term flood risks in a closed  
943 watershed. *Environ. Sci. Policy* 94, 112-122. <https://doi.org/10.1016/j.envsci.2018.12.032>,2019.

944 Güneralp, B., Güneralp, O. and Liu, Y.: Changing global patterns of urban exposure to flood and drought  
945 hazards. *Global Environmental Change*, 31: 217-225. <https://doi.org/10.1016/j.gloenvcha.2015.01.002>,  
946 2015.

947 Guo, H., Hu, Q., Zhang, Q.Feng, S.: Effects of the Three Gorges Dam on Yangtze River flow and river  
948 interaction with Poyang Lake, China: 2003-2008. *J. Hydrol.* 416, 19-27.  
949 <https://doi.org/10.1016/j.jhydrol.2011.11.027>,2012.

950 Gupta, H.V., Kling, H., Yilmaz, K.K.Martinez, G.F.: Decomposition of the mean squared error and NSE  
951 performance criteria: Implications for improving hydrological modelling. *J. Hydrol.* 377 (1-2), 80-91.  
952 <https://doi.org/10.1016/j.jhydrol.2009.08.003>,2009.

953 Hagemann, S. and Jacob, D.: Gradient in the climate change signal of European discharge predicted by a

954 multi-model ensemble. *Climatic Change*, 81(S1): 309-327. <https://doi.org/10.1007/s10584-006-9225-0>,  
955 2007.

956 Hallegatte, S., Green, C., Nicholls, R.J. and Corfee-Morlot, J.: Future flood losses in major coastal cities.  
957 *Nature climate change*, 3(9): 802-806. <https://doi.org/10.1038/nclimate1979>, 2013

958 Hirabayashi, Y. et al.: Global flood risk under climate change. *Nature Climate Change*, 3(9): 816-821.  
959 <https://doi.org/10.1038/nclimate1911>, 2013.

960 Hisdal, H. and Tallaksen, L.M.: Estimation of regional meteorological and hydrological drought  
961 characteristics: a case study for Denmark. *Journal of Hydrology*, 281(3): 230-247.  
962 [https://doi.org/10.1016/S0022-1694\(03\)00233-6](https://doi.org/10.1016/S0022-1694(03)00233-6), 2003.

963 Hutchinson, M.F. and Xu, T. Anusplin version 4.2 user guide. Centre for Resource and Environmental  
964 Studies. The Australian National University. Canberra, 5, 2004

965 Javaheri, A. and Babbar-Sebens, M.: On comparison of peak flow reductions, flood inundation maps, and  
966 velocity maps in evaluating effects of restored wetlands on channel flooding. *Ecological Engineering*, 73:  
967 132-145. <https://doi.org/10.1016/j.ecoleng.2014.09.021>, 2014.

968 Jongman, B.: Effective adaptation to rising flood risk. *Nat. Commun.* 9 (1), 1986.  
969 <https://doi.org/10.1038/s41467-018-04396-1>, 2018.

970 Kharrufa, N.S., 1985. Simplified equation for evapotranspiration in arid regions. *Hydrologie Sonderheft*, 5(1):  
971 39-47.

972 Kriegler, E., Bauer, N., Popp, A., Humpenöder, F., Leimbach, M., Strefler, J., Baumstark, L., Bodirsky, B.L.,  
973 Hilaire, J.Klein, D.: Fossil-fueled development (SSP5): An energy and resource intensive scenario for the  
974 21st century. *Global environmental change* 42, 297-315.  
975 <https://doi.org/10.1016/j.gloenvcha.2016.05.015>, 2017.

976 Kumar, P., Debele, S.E., Sahani, J., Rawat, N., Marti-Cardona, B., Alfieri, S.M., Basu, B., Basu, A.S.,  
977 Bowyer, P., Charizopoulos, N., Gallotti, G., Jaakko, J., Leo, L.S., Loupis, M., Menenti, M., Mickovski,  
978 S.B., Mun, S., Gonzalez-Ollauri, A., Pfeiffer, J., Pilla, F., Pröll, J., Rutzinger, M., Santo, M.A., Sannigrabi,  
979 S., Spyrou, C., Tuomenvirta, H.Zieher, T.: Nature-based solutions efficiency evaluation against natural  
980 hazards: Modelling methods, advantages and limitations. *Sci. Total Environ.* 784, 147058.  
981 <https://doi.org/10.1016/j.scitotenv.2021.147058>, 2021.

982 Lee, S., Yeo, I.Y., Lang, M.W., Sadeghi, A.M., Mccarty, G.W., Moglen, G.E.Evenson, G.R.: Assessing the  
983 cumulative impacts of geographically isolated wetlands on watershed hydrology using the SWAT model  
984 coupled with improved wetland modules. *J. Environ. Manage.* 223, 37-48.  
985 <https://doi.org/10.1016/j.jenvman.2018.06.006>,2018.

986 Liu, D.: A rational performance criterion for hydrological model. *J. Hydrol.* 590, 125488.  
987 <https://doi.org/10.1016/j.jhydrol.2020.125488>,2020.

988 Li, F., Zhang, G. and Xu, Y.J.: Spatiotemporal variability of climate and streamflow in the Songhua River  
989 Basin, northeast China. *Journal of Hydrology*, 514: 53-64. <https://doi.org/10.1016/j.jhydrol.2014.04.010>,  
990 2014.

991 Li, W., Jiang, Y., Duan, Y., Bai, J., Zhou, D.Ke, Y.: Where and how to restore wetland by utilizing storm  
992 water at the regional scale: A case study of Fangshan, China. *Ecol. Indic.* 122, 107246.  
993 <https://doi.org/https://doi.org/10.1016/j.ecolind.2020.107246>,2021.

994 Lobligeois, F., Andréassian, V., Perrin, C., Tabary, P., and Loumagne, C.: When does higher spatial  
995 resolution rainfall information improve streamflow simulation? An evaluation using 3620 flood events,  
996 *Hydrol. Earth Syst. Sci.*, 18, 575–594, <https://doi.org/10.5194/hess-18-575-2014>, 2014.

997 Maes, J., Barbosa, A., Baranzelli, C., Zulian, G., Batista E Silva, F., Vandecasteele, I., Hiederer, R., Liqueite,  
998 C., Paracchini, M.L., Mubareka, S., Jacobs-Crisioni, C., Castillo, C.P.Lavalle, C.: More green  
999 infrastructure is required to maintain ecosystem services under current trends in land-use change in  
1000 Europe. *Landsc. Ecol.* 30 (3), 517-534. <https://doi.org/10.1007/s10980-014-0083-2>,2015.

1001 Manfreda, S., Miglino, D., and Albertini, C.: Impact of detention dams on the probability distribution of  
1002 floods, *Hydrol. Earth Syst. Sci.*, 25, 4231–4242, <https://doi.org/10.5194/hess-25-4231-2021>, 2021.

1003 Maraun, D.: Bias Correcting Climate Change Simulations - a Critical Review. *Current Climate Change*  
1004 *Reports*, 2(4): 211-220. <https://doi.org/10.1007/s40641-016-0050-x>, 2016.

1005 Martinez-Martinez, E., Nejadhashemi, A.P., Woznicki, S.A.Love, B.J.: Modeling the hydrological  
1006 significance of wetland restoration scenarios. *J. Environ. Manage.* 133, 121-134.  
1007 <https://doi.org/10.1016/j.jenvman.2013.11.046>,2014.

1008 Melsen, L.A., Teuling, A.J., Torfs, P.J.J.F., Zappa, M., Mizukami, N., Mendoza, P.A., Clark, M.P.Uijlenhoet,  
1009 R.: Subjective modeling decisions can significantly impact the simulation of flood and drought events. *J.*

1010 Hydrol. 568, 1093-1104. <https://doi.org/10.1016/j.jhydrol.2018.11.046>,2019.

1011 Meng, B., Liu, J., Bao, K., Sun, B.: Water fluxes of Nenjiang River Basin with ecological network analysis:  
1012 Conflict and coordination between agricultural development and wetland restoration. *J. Clean. Prod.* 213,  
1013 933-943. <https://doi.org/10.1016/j.jclepro.2018.12.243>,2019.

1014 Moore, K., Pierson, D., Pettersson, K., Schneiderman, E. and Samuelsson, P.: Effects of warmer world  
1015 scenarios on hydrologic inputs to Lake Mälaren, Sweden and implications for nutrient loads.  
1016 *Hydrobiologia*, 599(1): 191-199. [https://doi.org/10.1007/978-1-4020-8379-2\\_23](https://doi.org/10.1007/978-1-4020-8379-2_23), 2008.

1017 Moriasi, D.N.: Model Evaluation Guidelines for Systematic Quantification of Accuracy in Watershed  
1018 Simulations. *Trans. ASABE* 50 (3), 885-900. <https://doi.org/10.13031/2013.23153>,2007.

1019 Moriasi, D.N., Gitau, M.W., Pai, N. and Daggupati, P.: Hydrologic and water quality models: Performance  
1020 measures and evaluation criteria. *Transactions of the ASABE*, 58(6): 1763-1785.  
1021 [10.13031/trans.58.10715](https://doi.org/10.13031/trans.58.10715), 2015

1022 Muller, M.: Hydropower dams can help mitigate the global warming impact of wetlands. *Nature* 566 (7744),  
1023 315-317. <https://doi.org/10.1038/d41586-019-00616-w>,2019.

1024 Nash, J.E. and Sutcliffe, J.V.: River flow forecasting through conceptual models part I—A discussion of  
1025 principles. *Journal of hydrology*, 10(3): 282-290. [https://doi.org/10.1016/0022-1694\(70\)90255-6](https://doi.org/10.1016/0022-1694(70)90255-6), 1970.

1026 Nelson, D.R., Bledsoe, B.P., Ferreira, S. and Nibbelink, N.P.: Challenges to realizing the potential of nature-  
1027 based solutions. *Current Opinion in Environmental Sustainability*, 45: 49-55.  
1028 <https://doi.org/10.1016/j.cosust.2020.09.001>, 2020.

1029 Nika, C.E., Gusmaroli, L., Ghafourian, M., Atanasova, N., Buttiglieri, G., Katsou, E.: Nature-based solutions  
1030 as enablers of circularity in water systems: A review on assessment methodologies, tools and indicators.  
1031 *Water Res.* 183, 115988. <https://doi.org/10.1016/j.watres.2020.115988>,2020.

1032 Noël, P., Rousseau, A.N., Paniconi, C. and Nadeau, D.F.: Algorithm for delineating and extracting hillslopes  
1033 and hillslope width functions from gridded elevation data. *Journal of Hydrologic Engineering*, 19(2):  
1034 366-374. [https://doi.org/10.1061/\(ASCE\)HE.1943-5584.000007](https://doi.org/10.1061/(ASCE)HE.1943-5584.000007), 2014.

1035 O'Neill, B. C., Tebaldi, C., van Vuuren, D. P., Eyring, V., Friedlingstein, P., Hurtt, G., Knutti, R., Kriegler,  
1036 E., Lamarque, J.-F., Lowe, J., Meehl, G. A., Moss, R., Riahi, K., and Sanderson, B. M.: The Scenario  
1037 Model Intercomparison Project (ScenarioMIP) for CMIP6, *Geosci. Model Dev.*, 9, 3461–3482,

1038 <https://doi.org/10.5194/gmd-9-3461-2016>, 2016.

1039 Park, J., Botter, G., Jawitz, J.W. and Rao, P.S.C.: Stochastic modeling of hydrologic variability of  
1040 geographically isolated wetlands: Effects of hydro-climatic forcing and wetland bathymetry. *Advances*  
1041 *in Water Resources*, 69: 38-48. <https://doi.org/10.1016/j.advwatres.2014.03.007>, 2014.

1042 Pool, S., Vis, M., Seibert, J.Sveriges, L.: Evaluating model performance: towards a non-parametric variant  
1043 of the Kling-Gupta efficiency. *Hydrological sciences journal* 63 (13-14), 1941-1953.  
1044 <https://doi.org/10.1080/02626667.2018.1552002>,2018.

1045 Rajib, A., Golden, H.E., Lane, C.R.Wu, Q.: Surface Depression and Wetland Water Storage Improves Major  
1046 River Basin Hydrologic Predictions. *Water Resour. Res.* 56 (7), e2019WR026561.  
1047 <https://doi.org/https://doi.org/10.1029/2019WR026561>,2020.

1048 Rousseau, A.N., Fortin, J., Turcotte, R., Royer, A., Savary, S., Quévy, F., Noël, P.Paniconi, C.: PHYSITEL,  
1049 a specialized GIS for supporting the implementation of distributed hydrological models. *Water News-*  
1050 *Official Magazine of the Canadian Water Resources Association* 31 (1), 18-20, 2011.

1051 Saharia, M. et al.: Mapping Flash Flood Severity in the United States. *Journal of Hydrometeorology*, 18(2):  
1052 397-411. <https://doi.org/10.1175/JHM-D-16-0082.1>, 2017.

1053 Schneider, C., Flörke, M., De Stefano, L.Petersen-Perlman, J.D.: Hydrological threats to riparian wetlands  
1054 of international importance – a global quantitative and qualitative analysis. *Hydrol. Earth Syst. Sci.* 21  
1055 (6), 2799-2815. <https://doi.org/10.5194/hess-21-2799-2017>,2017.

1056 Seibert, J., Vis, M.J.P., Lewis, E. and Meerveld, H.J.: Upper and lower benchmarks in hydrological modelling.  
1057 *Hydrological Processes*, 32: 1120 - 1125. <https://doi.org/10.1002/hyp.11476>, 2018.

1058 Shafeeque, M. and Luo, Y.: A multi-perspective approach for selecting CMIP6 scenarios to project climate  
1059 change impacts on glacio-hydrology with a case study in Upper Indus river basin. *Journal of Hydrology*,  
1060 599: 126466. <https://doi.org/10.1016/j.jhydrol.2021.126466>, 2021.

1061 Shook, K., Papalexioiu, S.Pomeroy, J.W.: Quantifying the effects of Prairie depressional storage complexes  
1062 on drainage basin connectivity. *J. Hydrol.* 593, 125846.  
1063 <https://doi.org/https://doi.org/10.1016/j.jhydrol.2020.125846>,2021.

1064 Smakhtin, V.U., 2001. Low flow hydrology: a review. *Journal of Hydrology*, 240(3): 147-186.  
1065 [https://doi.org/10.1016/S0022-1694\(00\)00340-1](https://doi.org/10.1016/S0022-1694(00)00340-1), 2001.

1066 Staudinger, M., Stahl, K., Seibert, J., Clark, M. P., and Tallaksen, L. M.: Comparison of hydrological model  
1067 structures based on recession and low flow simulations, *Hydrol. Earth Syst. Sci.*, 15, 3447–3459,  
1068 <https://doi.org/10.5194/hess-15-3447-2011>, 2011.

1069 Tallaksen, L.M. and van Lanen, H.A.J.: Hydrological drought; processes and estimation methods for  
1070 streamflow and groundwater. *Developments in water science*, 48, 2004.

1071 Thorslund, J., Jarsjo, J., Jaramillo, F., Jawitz, J.W., Manzoni, S., Basu, N.B., Chalov, S.R., Cohen, M.J.,  
1072 Creed, I.F., Goldenberg, R., Hylin, A., Kalantari, Z., Koussis, A.D., Lyon, S.W., Mazi, K., Mard, J.,  
1073 Persson, K., Pietro, J., Prieto, C., Quin, A., Van Meter, K., Destouni, G.: Wetlands as large-scale nature-  
1074 based solutions: Status and challenges for research, engineering and management. *Ecol. Eng.* 108, 489-  
1075 497. <https://doi.org/https://doi.org/10.1016/j.ecoleng.2017.07.012,2017>.

1076 Tolson, B.A. and Shoemaker, C.A.: Dynamically dimensioned search algorithm for computationally efficient  
1077 watershed model calibration. *Water Resources Research*, 43(1): 1-6.  
1078 <https://doi.org/10.1029/2005WR004723>, 2007.

1079 Turcotte, R., Fortin, L.G., Fortin, V., Fortin, J.P. and Villeneuve, J.P.: Operational analysis of the spatial  
1080 distribution and the temporal evolution of the snowpack water equivalent in southern Québec, Canada.  
1081 *Hydrology Research*, 38(3): 211-234. <https://doi.org/10.2166/nh.2007.009>, 2007.

1082 UNISDR, C. The human cost of natural disasters: A global perspective, 2015.

1083 Van Vuuren, D. P., Riahi, K., Calvin, K., Dellink, R., Emmerling, J., Fujimori, S., O'Neill, B.: The Shared  
1084 Socio-economic Pathways: Trajectories for human development and global environmental change.  
1085 *Global Environmental Change*, 42: 148-152. <http://dx.doi.org/10.1016/j.gloenvcha.2016.10.009>, 2017.

1086 Walz, Y., Janzen, S., Narvaez, L., Ortiz-Vargas, A., Woelki, J., Doswald, N., & Sebesvari, Z.: Disaster-  
1087 related losses of ecosystems and their services. Why and how do losses matter for disaster risk reduction?  
1088 *International Journal of Disaster Risk Reduction*, 63: 102425. <https://doi.org/10.1016/j.ijdrr.2021.102425>,  
1089 2021.

1090 Wang, L., Chen, X., Shao, Q. and Li, Y.: Flood indicators and their clustering features in Wujiang River,  
1091 South China. *Ecological Engineering*, 76: 66-74. <https://doi.org/10.1016/j.ecoleng.2014.03.018>, 2015.

1092 Wang, S., Zhang, L., She, D., Wang, G., Zhang, Q.: Future projections of flooding characteristics in the  
1093 Lancang-Mekong River Basin under climate change. *J. Hydrol.* 602, 126778.

1094 <https://doi.org/10.1016/j.jhydrol.2021.126778>,2021.

1095 Wang, X.: Using Hydrologic Equivalent Wetland Concept Within SWAT to Estimate Streamflow in  
1096 Watersheds with Numerous Wetlands. *Trans. ASABE* 51 (1), 55-72.  
1097 <https://doi.org/10.13031/2013.24227>,2008.

1098 Ward, P.J., de Ruiter, M.C., Mård, J., Schröter, K., Van Loon, A., Veldkamp, T., von Uexkull, N., Wanders,  
1099 N., Aghakouchak, A., Arnbjerg-Nielsen, K., Capewell, L., Carmen Llasat, M., Day, R., Dewals, B., Di  
1100 Baldassarre, G., Huning, L.S., Kreibich, H., Mazzoleni, M., Savelli, E., Teutschbein, C., van den Berg,  
1101 H., van der Heijden, A., Vincken, J.M.R., Waterloo, M.J.Wens, M.: The need to integrate flood and  
1102 drought disaster risk reduction strategies. *Water Security* 11, 100070.  
1103 <https://doi.org/10.1016/j.wasec.2020.100070>,2020.

1104 Wu, Y., Zhang, G., Rousseau, A.N.Xu, Y.J.: Quantifying streamflow regulation services of wetlands with an  
1105 emphasis on quickflow and baseflow responses in the Upper Nenjiang River Basin, Northeast China. *J.*  
1106 *Hydrol.* 583, 124565. <https://doi.org/10.1016/j.jhydrol.2020.124565>,2020. Wu, Y., Zhang, G., Rousseau,  
1107 A.N., Xu, Y.J. and Foulon, É., 2020. On how wetlands can provide flood resilience in a large river basin:  
1108 A case study in Nenjiang river Basin, China. *Journal of Hydrology*, 587: 125012.

1109 Wu, Y., Zhang, G., Xu, Y.J.Rousseau, A.N.: River Damming Reduces Wetland Function in Regulating Flow.  
1110 *J. Water Resour. Plan. Manage.-ASCE* 147 (10), 05021014. [https://doi.org/10.1061/\(ASCE\)WR.1943-](https://doi.org/10.1061/(ASCE)WR.1943-)  
1111 [5452.0001434](https://doi.org/10.1061/(ASCE)WR.1943-5452.0001434),2021.

1112 Xu, X., Wang, Y. C., Kalcic, M., Muenich, R. L., Yang, Y. E., & Scavia, D.: Evaluating the impact of climate  
1113 change on fluvial flood risk in a mixed-use watershed. *Environmental modelling & software*, 122, 104031.  
1114 <https://doi.org/10.1016/j.envsoft.2017.07.013>, 2019.

1115 Yassin, F., Razavi, S., Elshamy, M., Davison, B., Sapriza-Azuri, G., and Wheeler, H.: Representation and  
1116 improved parameterization of reservoir operation in hydrological and land-surface models, *Hydrol. Earth*  
1117 *Syst. Sci.*, 23, 3735–3764, <https://doi.org/10.5194/hess-23-3735-2019>, 2019.

1118 Zedler, J.B.Kercher, S.: WETLAND RESOURCES: Status, Trends, Ecosystem Services, and Restorability.  
1119 *Annu. Rev. Environ. Resour* 30 (1), 39-74.  
1120 <https://doi.org/10.1146/annurev.energy.30.050504.144248>,2005.

1121 Zelenhasić, E. and Salvai, A., 1987. A method of streamflow drought analysis. *Water resources research*,

1122 23(1): 156-168. <https://doi.org/10.1029/WR023i001p00156>, 1987.

1123 Zeng, L., Shao, J.Chu, X.: Improved hydrologic modeling for depression-dominated areas. *J. Hydrol.* 590,  
1124 125269. <https://doi.org/https://doi.org/10.1016/j.jhydrol.2020.125269,2020>.

1125 Zhang, X.Song, Y.: Optimization of wetland restoration siting and zoning in flood retention areas of river  
1126 basins in China: A case study in Mengwa, Huaihe River Basin. *J. Hydrol.* 519, 80-93.  
1127 <https://doi.org/10.1016/j.jhydrol.2014.06.043,2014>.

1128 Zhao, G., Gao, H., Naz, B.S., Kao, S.Voisin, N.: Integrating a reservoir regulation scheme into a spatially  
1129 distributed hydrological model. *Adv. Water Resour.* 98, 16-31.  
1130 <https://doi.org/10.1016/j.advwatres.2016.10.014,2016>.

1131 Zhao, Y., Dong, N., Li, Z., Zhang, W., Yang, M.Wang, H.: Future precipitation, hydrology and hydropower  
1132 generation in the Yalong River Basin: Projections and analysis. *J. Hydrol.* 602, 126738.  
1133 <https://doi.org/10.1016/j.jhydrol.2021.126738,2021>.